AD-A151 796
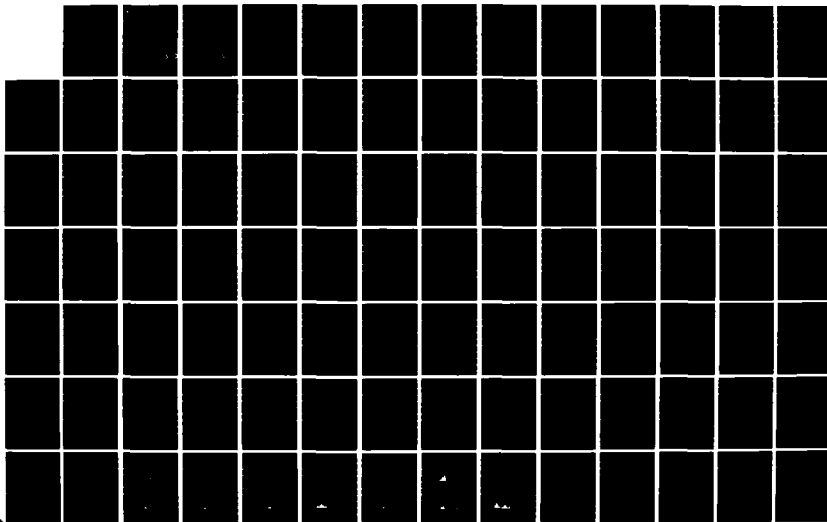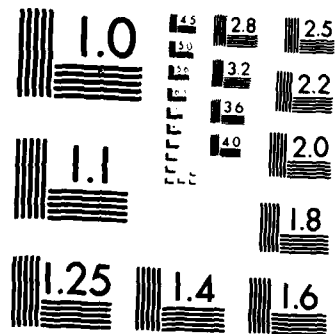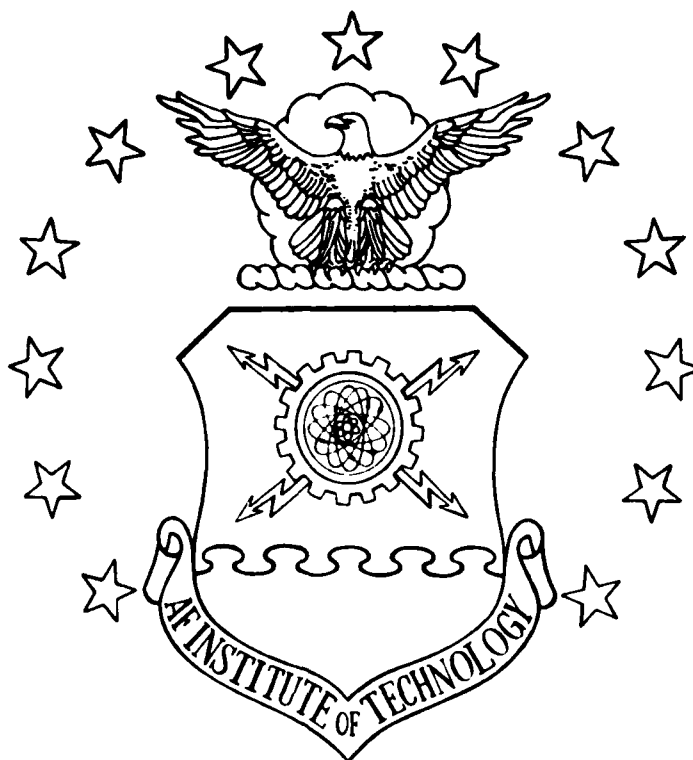
INVESTIGATION OF ELECTRON ATTACHMENT AND
DISSOCIATION RATES IN C_3F_8/CH_4 ELECTRIC
GAS DISCHARGES

THESIS

Carl R. Wilson
First Lieutenant, USAF

AFIT/GEO/PH/84D-5

DTIC
ELECTE
MAR 2 9 1985
S   D
B

DEPARTMENT OF THE AIR FORCE

AIR UNIVERSITY

AIR FORCE INSTITUTE OF TECHNOLOGY

Wright-Patterson Air Force Base, Ohio

85   03   13   186

INVESTIGATION OF ELECTRON ATTACHMENT AND
DISSOCIATION RATES IN C_3F_6/CH_4 ELECTRIC
GAS DISCHARGES

THESIS

Verl R. Wilson
First Lieutenant, USAF

AFIT/GEO/PH/84D-5

DTIC
ELECTED
MAR 2 9 1985

B

AFIT/GEO/PH/84D-5

INVESTIGATION OF ELECTRON ATTACHMENT AND DISSOCIATION RATES
IN C_2F_5/CH_4 ELECTRIC GAS DISCHARGES

THESIS

Presented to the Faculty of the School of Engineering
of the Air Force Institute of Technology
Air University
In Partial Fulfillment of the
Requirements for the Degree of
Master of Science in Electrical Engineering

Verl R. Wilson, B.S.
First Lieutenant, USAF

December 1984

PREFACE

There are certain aspects of any study which stand out as particularly important to the individual performing the study. For me the most difficult and rewarding tasks were those involving the interpretation of results. The culmination of years of classroom training and lab experimentation is when the student performs on his own to glean new and useful information out of a detailed experiment. I am indeed fortunate to have had this opportunity to develop my own skills and experience true lab work first hand.

The support I received during the accomplishment of this work was truly superior. I am grateful to my faculty advisor, Lt Col William F. Bailey, for the precious hours he devoted to my understanding. Also, to Capt Greg Schneider, whose previous work in gas discharges served as the outline for my own. To Dr. Alan Garscaden, Mr. Robert Knight, and Lt Pete Haaland at the Energy Conversion Branch of the Air Force Aero Propulsion Laboratory, for technical and theoretical support, I give my sincere thanks. My warmest thanks goes to my mentor, teacher, and lab advisor, Dr Peter Bletzinger, without whose guidance, patience, and understanding I would surely have failed. Lastly, I would like to thank my wife, Wanna, and my two boys, Daryl and Dennis, for their love and support and for the unselfish sacrifices they gave to the completion of this work.

Verl R. Wilson

Contents

Contents

Accession For

NTIS

DT

U

J

D   tion/

Availability Codes

Avail and/or

Dist   Special

A-1

DTIC
COPY
INSPECTED
1

List of Figures

List of Figures

List of Tables

List of Symbols [2:vii]

A	Collector area (cm^2)
A	Ampere
cm	Centimeter
CW	Continuous wave
dE/dm	Mean stopping power of gas (eV cm^2/g)
e	Electronic charge (1.6×10^{-19} Coulomb)
e	Electron
E	Electric field strength (V/cm)
E_i	Effective ionization potential (V)
eV	Electron volt
F	Farad
g	Gram
h	Planck's constant (6.626×10^{-34} Joule-sec)
Hz	Hertz
I	Current (Amperes)
j	Current density (A/cm^2)
j_{eb}	Electron beam current density (A/cm^2)
k_i	Ion-ion recombination rate (cm^3/sec)
kV	Kilovolt
kW	Kilowatt
M	Mean gas molecular weight (g)
mA	Milliampere
m_p	Mass of proton (1.67×10^{-24} g)
mm	Millimeter
N	Neutral gas number density (cm^{-3})

n_a	Number density of attaching species (cm^{-3})
n_e	Number density of electrons (cm^{-3})
n_{eo}	Number density of electron at steady-state (cm^{-3})
n_f	Final number density of electrons (cm^{-3})
n_-	Number density of negative ions (cm^{-3})
n_+	Number density of positive ions (cm^{-3})
S	Electron beam electron-ion pair porduction rate (sec^{-1})
t	Time (sec)
T_d	Townsend (1×10^{-17} V-cm^2)
T_e	Electron temperature (eV)
V	Volt
w_e	Electron drift velocity (cm/sec)
w_-	Negative ion drift velocity (cm/sec)
w_+	Positive ion drift velocity (cm/sec)
z	Townsend ionization coefficient (cm^{-1})
α	Electron-ion recombination rate (cm^3/sec)
β	Attachment rate (sec^{-1})
k_a	Attachment coefficient (cm^3/sec)
μ	Micro (10^{-6})
f	Frequency (sec^{-1})
σ	Diffusion coefficient (cm^2/sec)
*	Excited species
$^\circ$C	Degrees centigrade
$^\circ$K	Degrees Kelvin
-	Negative charge
+	Positive charge

Abstract

This investigation determined the attachment and dissociation rates of the electronegative gas, C_2F_6, in a buffer gas of methane at atmospheric pressure when undergoing electron-beam sustained gas discharges. A non-linear least-squares fit of the electron lifetime equation to the decay portion of the discharge current pulse indicates an attachment rate of 5×10^5 sec^{-1} for a gas mixture ratio of 0.1/755, C_2F_6/CH_4 and an E/N range of 4 to 13 Townsend. Results of the curve fit were inconclusive for E/N below 4 Townsend due to the effects of a slowly decaying electron-beam. Attempts were made to measure the dissociation rate of C_2F_6 as a function of discharge time at an E/N equal to 13 Townsend using a residual gas analyzer. The actual dissociation rate was not determined. However, it was confirmed that the dissociation of C_2F_6 due to electron-beam pulses and gas discharges is not significant in large closed-cycle gas flow loops as proposed for pulsed power switching if E/N is held below 13 Townsend.

INVESTIGATION OF ELECTRON ATTACHMENT AND DISSOCIATION RATES IN C_2F_6/CH_4 ELECTRIC GAS DISCHARGES

I. Introduction

There is currently considerable interest in using inductive storage devices for storing and rapidly transferring electrical energy to pulsed power systems. Inductive energy storage is attractive in pulsed power applications due to the inductor's intrinsically high energy storage capability (100 to 1000 times that of comparable capacitive systems) [1]. The increase in energy storage capability translates into increased design flexibility and portability for both military and commercial pulsed power systems. The key to using inductive energy discharge systems, especially for repetitive operation (repetition rates $>10^3$ pulses per sec in short bursts) and long lifetimes (more than 10^5 bursts), is the switch used to open the charging circuit and transfer the stored power to the using device.

One of the most promising contenders for fast repetitive switching is an electron-beam (e-beam) controlled diffuse gas discharge switch operating at a gas pressure of one or more atmospheres (see Figure 1). This switch promises to have the desirable switching characteristics of high current conductivity during the on phase, very high impedance during the off phase, fast switching action between the on and off phases, and a long life expectancy. Operation begins when

1
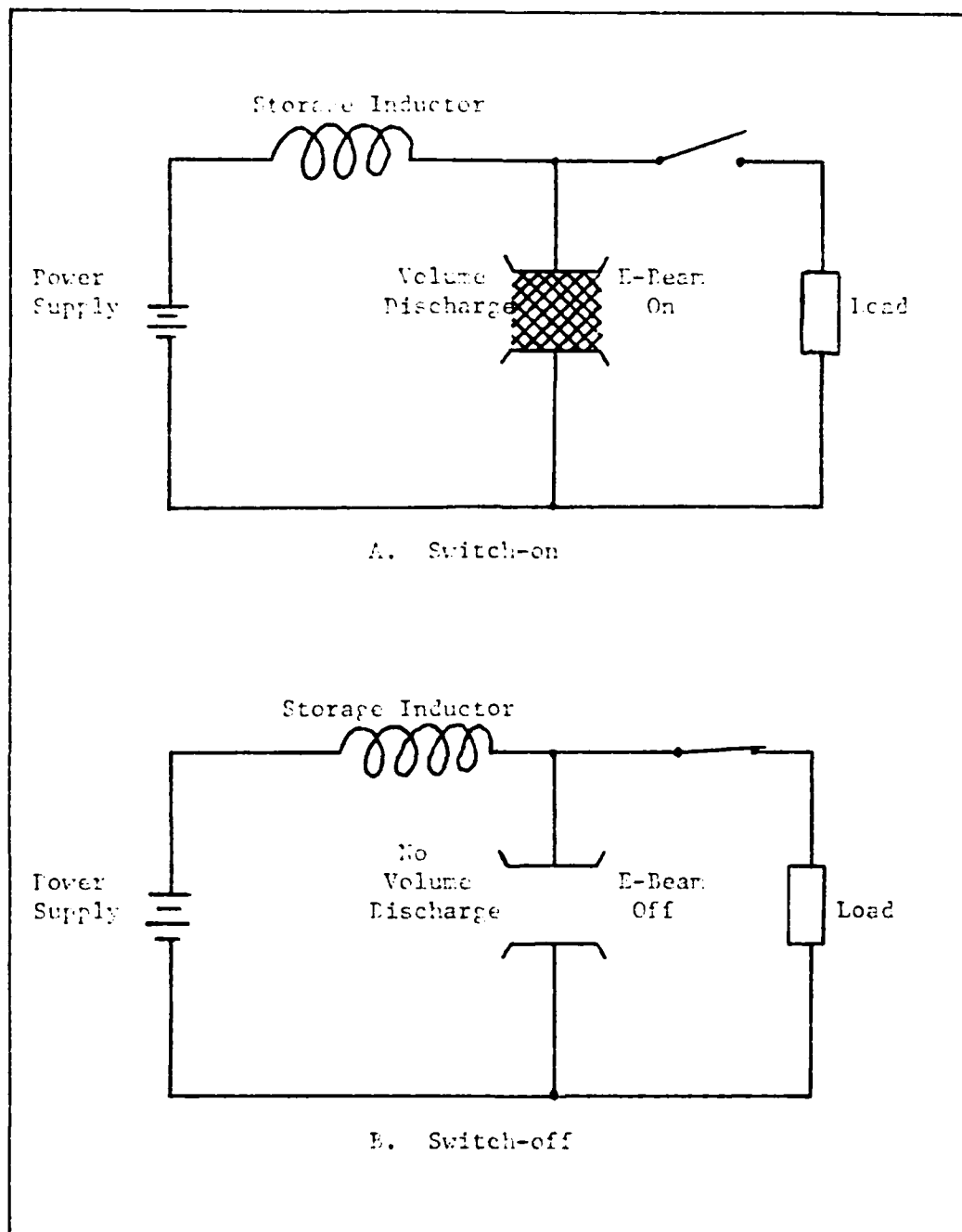
Figure 1. Schematic of E-Beam Switch Operation

an ionizing e-beam is fired into the gas between the electrodes. The high energy e-beam electrons cause ionization of the gas creating a plasma which conducts (switch turn-on phase) expanding the fields about the inductor. When the e-beam is turned-off, the conductivity of the plasma decreases, due to recombination and attachment processes (switch turn-off phase), the fields about the inductor collapse, and a large current pulse is sent through the load. It is easily seen that the performance of the switch is strongly dependent on the gas mixture used in the gas discharge chamber.

It is particularly important that free electrons be quickly removed from the plasma during the switch opening phase so that the conductivity of the switch is rapidly reduced to zero (switch open), thus, transferring maximum pulsed power to the load (power goes as the time rate of change in current). On the contrary, it is desirable to have as many free electrons as possible in the plasma during the on phase so that a high conductivity is maintained. Several gas mixtures have been investigated which use a small amount of attaching gas, whose attachment rate is dependent on E/N (electric field-to-neutral gas density ratio), in a relatively large amount of pure buffer gas to enhance switching operation. The E/N dependent attaching gas has a high electron attachment rate at the high E/N values experienced during the opening-phase and a much lower electron attachment rate at the low E/N values

characteristic of the conducting phase of switch operation. The following work was performed to gain additional experimental knowledge concerning one of the more promising attaching gases, hexafluoroethane (C_2F_6), mixed with a buffer gas of methane.

Problem

The original objective of this experiment was to investigate the suitability of the electronegative (attaching) gases hexafluoroethane (C_2F_6), perfluoropropane (C_3F_8), and tetrafluoromethane (CF_4) each in a buffer gas of pure methane as possible e-beam switching gas mixtures. Due to the time constraints imposed, only the attaching gas C_2F_6 in pure methane was experimentally investigated for the E/N range of .2 to 13 Townsend and for the attaching to buffer gas ratio of 0.1 to 755 torr respectively (reduced to 700 torr total pressure). The following properties of the gas were to be investigated and compared to published and theoretical results:

1. Dissociation rate of the attaching gas as a function of discharge current, E/N, and number of operations.

2. The change in composition of the gas mixture as a function of time and discharge current using a residual gas analyzer.

3. The attachment rate of the gas mixture at the low E/N values of between .2 and 13 Townsend.

4

Assumptions

To aid in mathematically modeling the experiment, certain assumptions were made during the course of this experiment. The assumptions are reasonable in light of published literature [2:1-23,3:4-9], and are as follows:

1. Electron diffusion losses inside the gas chamber will be assumed negligible since the chamber is relatively large (on the order of centimeters) and the operational pressure of the system high (greater than 1-atmosphere)

2. The gas plasma will be assumed spatially uniform and electrically neutral, i.e., number of electrons plus the number of negative ions will equal the number of positive ions. This is reasonable since the chamber dimensions will be much greater than a Debye length.

3. The electric field, E, across the discharge chamber will be assumed uniformly distributed and constant with time (except for the relatively narrow cathode-fall region discussed later).

4. The amount of gas removed from the system for sampling by an on-line residual gas analyzer will be assumed negligible compared to the total gas in the system.

5. The influence of the attaching gas on the electron energy distribution function is assumed negligible since the partial pressure of the attaching gas is extremely small (less than 1/7550) with respect to the buffer gas. Therefore, the drift velocity of the gas mixture is assumed to be that of the buffer gas, methane, which is well known [3:17,4].

These assumptions will be more fully discussed in later sections of this report where applicable.

Standards

Test runs were conducted at known operating ranges of e-beam current, discharge current, and gas mixtures to ob-

tain data for comparison with previously obtained results using similar equipment. Also, tests were conducted with pure methane in the discharge chamber over the same operating ranges expected for the switch gas mixture. These served as the departure point from which to begin the proposed experiment and gather new data.

Approach

The fundamental approach was to strike an e-beam sustained discharge in a quartz-lined stainless-steel chamber within a closed-cycle gas flow loop. Next, the discharge current and discharge voltage was to be measured using a high speed programmable digitizer and recorded using a Hewlett-Packard 9826 computer. By maintaining a constant e-beam current, varying the anode-cathode distance and keeping the discharge current constant through adjustment of the discharge voltage in the manner described by Bletzinger [5:38], the cathode-fall voltage was to be determined for each operating range of interest. Also, by performing a non-linear least-squares fit of the electron density equation [6:4821-4822], to the decay portion of the recorded discharge current pulses, the attachment rate coefficient was to be determined for a variety of discharge voltages and e-beam currents at fixed anode-cathode distances. From this reduced data a plot of the attachment rate as a function of E/N for the range of .2 to 13 Townsend was to be performed.

6

Two methods were to be used to determine the rate of dissociation of the attaching gas as a function of time and size of discharge. The first was to use a residual gas analyzer, Inficon IQ-200, to detect the relative gas composition at different stages of operation and compute the dissociation rate based on the relative amount of selected negative ions in the gas compared to those present in the virgin gas. The second method was to monitor and record the discharge current curve at regular interval over approximately 300,000 four-microsecond pulses at maximum e-beam current (1 amp before foil) and maximum switch voltage (10 kv). Next, the attachment rate for each discharge current pulse was to be calculated, as above, and the change in attachment over the 300,000 pulses computed. The rate of change in attachment would then be directly related to the dissociation rate of the attaching gas.

Sequence of Presentation

The presentation will start with a general background treatise to explain important gas discharge characteristics, such as structure, electron-ion formation and loss processes, and types of chemical reactions occurring within a dense gas. Then, a theoretical description of the plasma in mathematical terms will be reviewed, where special emphasis will be given to specific theory used in this investigation. Next, the experimental equipment, set-up, and procedures will be discussed in detail outlining the peculiarities of

7

this particular experiment and some of the difficulties encountered in its performance. Fourth, the results of the investigation will be analyzed and compared with other studies and predicted results. Finally, the conclusions arrived at during the study and the recommendations for future studies will be presented.

The Gas Discharge

At atmospheric pressure, room temperature and in the absence of external forces, most gases are electrically neutral. That is, in the natural state, most gases contain too few ions and free electrons to conduct electricity. Therefore, the gas must acquire additional charge carriers from an external source and/or from internal ionization of the gas molecules before current conduction can occur. When the number of ions and free electrons increases sufficiently, the gas becomes a plasma able to conduct electricity when an electric field is impressed across it.

A plasma is, in a macroscopic sense, electrically neutral if two conditions are met. The first condition for electrical neutrality is that the plasma dimensions be much greater than a Debye length or electrostatic screening distance. The Debye length, λ_D, can be calculated from

$$\lambda^2_D = (2kT_e\epsilon_o)/(n_ee^2) \qquad\qquad [7:159] \quad (2.1)$$

where

$\qquad$ k = Boltzman's constant (1.38×10^{-23} J/$^{\circ}$K)

$\qquad T_e$ = average electron temperature of the gas ($^{\circ}$K)

$\qquad n_e$ = electron number density (cm^{-3})

$\qquad \epsilon_o$ = permittivity of free space (8.85×10^{-14} F/cm)

$\qquad$ e = charge on an electron (1.602×10^{-19} C)

9

The other condition for electrical neutrality is that there be many electrons within a sphere of radius λ_D. For the gas study conducted here T_e ranged from 300 to 9000 (.2 to 1.3 eV) degrees Kelvin and n_e ranged from 10^{11} to 10^{12} per cm^3. Therefore, λ_D was 1.2×10^{-4} to 2.7×10^{-3} or much less than the smallest dimension of the discharge chamber of 2.2 cm, thus satisfying the first condition. Also, within a sphere of radius λ_D there are greater than 4×10^3 electrons, which satisfies the second condition for a neutral plasma. Since the two conditions for electrical neutrality were satisfied for this experiment, the plasma was assumed to be electrically neutral throughout the discharge region.

There are essentially three types of gas discharges in the steady state. These are the Townsend or dark discharge, the glow discharge, and the arc discharge. During ionization by the e-beam, the gas discharge is that of a high pressure (>= 1 atm) glow discharge and its generic features are shown in Figure 2. As seen in Figure 2, the cathode-fall region is typically very narrow in a high-pressure glow discharge, but plays a significant role in this study due to the high potential drop across the region. The cathode-fall region is a result of very large fields (orders of magnitude greater than those in the positive column) due to a high concentration of ions. The large fields are necessary for the emission of electrons by the cathode, but because the region is so narrow in the axial
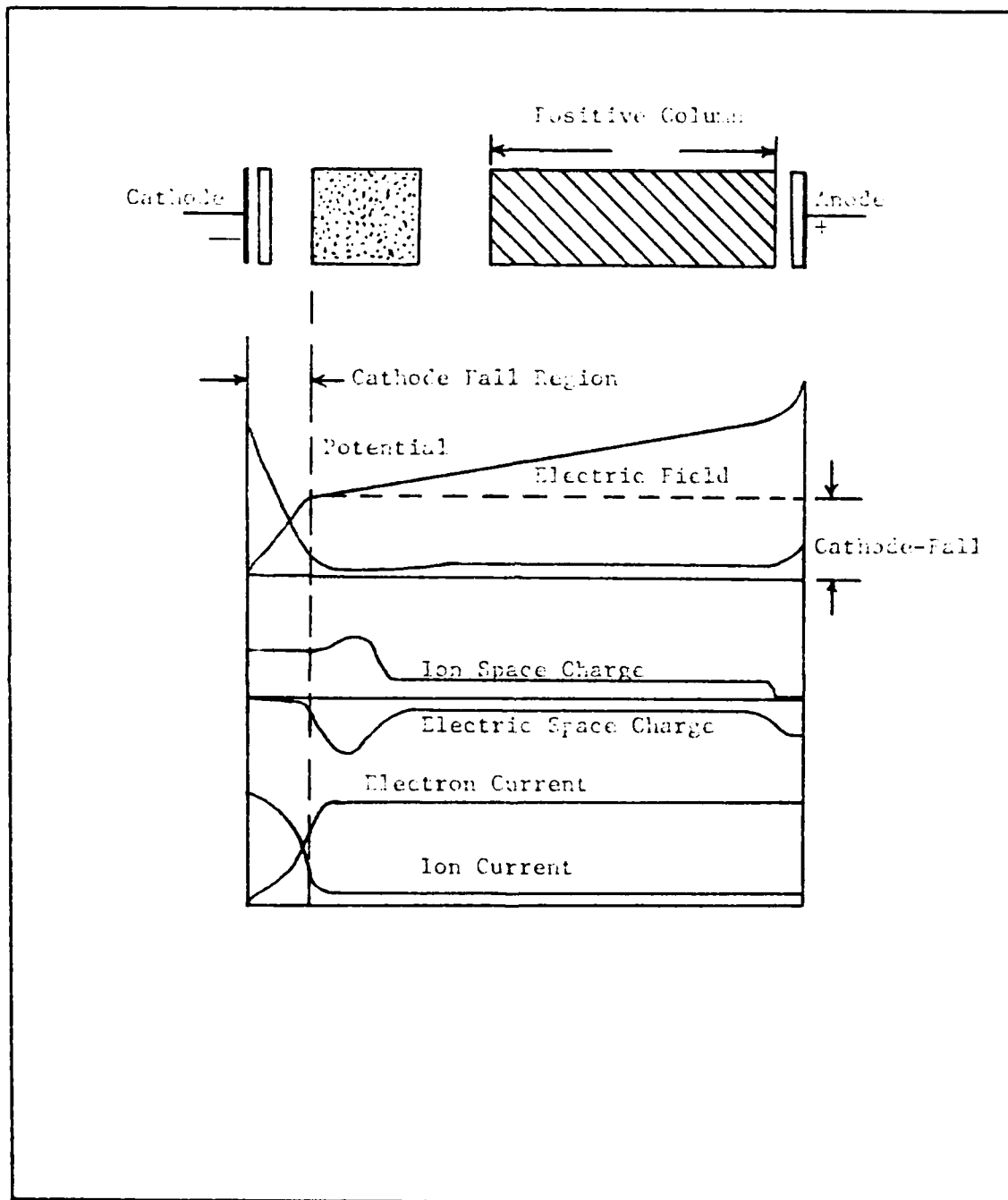
Figure 2. Structure of a Glow Discharge [8:218]

11

direction at atmospheric pressure, its main contribution is in lowering significantly the potential across the positive column region (a range of cathode-fall potentials from a few hundred volts to several thousand volts were experienced in this study). In this study the cathode-fall voltage was assumed to be constant for a constant e-beam current and voltage and for a constant E/N. However, the cathode-fall voltage is expected to increase slightly as the conductivity of the gas decreases following e-beam turned off.

The overwhelming majority of space between the electrodes is made up of the positive column (see Figure 2). Therefore, it is in this region that most of the electron-ion-neutral particle collision processes occur, such as ionization, electron attachment, and recombination. In the positive column, the electric field, charge density, and current density are virtually constant in the axial direction so that nearly the entire region formed between the electrodes is a relatively homogeneous medium. It is possible, however, for the properties of the positive column region to become oscillatory with respect to axial distance at certain values of E/N. This can cause discharge current and voltage oscillations across the discharge [9,10].

Fundamental Processes

In a gas discharge, current is conducted through a plasma from one electrical potential to another. However, to support a gas discharge, it is first necessary to form a

12

plasma with a large number of charged particles, ions and electrons. This is accomplished using an external source and/or through ionization of the medium itself. This section will describe the production and loss processes relevant to electric gas discharges.

A simple circuit analysis of a gas discharge yields the current density in the axial direction as

$$j = (n_e w_e + n_- w_- + n_+ w_+)e \qquad\qquad [3:5] \ (2.2)$$

where

j = current density in the axial direction (amps/cm^2)

n_e, n_-, n_+ = number density of electrons, positive and negative ions, which are traveling with components in the axial direction (cm^{-3})

w_e, w_-, w_+ = drift velocity of electrons, positive and negative ions, respectively (cm/sec)

e = electronic charge (1.602 x 10^{-19} C)

The above equation assumes that the only significant flow of charged particles is in the axial direction from one electrode to another. This is reasonable for high pressure gases and large chamber dimensions as will be seen later during the discussion on diffusion. Since the force due to the charge on each ion and electron are of the same magnitude, their drift velocities are inversely proportional to their respective masses. Also, the drift velocity is directly proportional to the time between collisions, τ_d, of the particle. In mathematical form the drift velocity, w,

13

for each particle is proportional to the ratio of τ_d to its respective mass.

$$w \propto \tau_d/M$$

where

w = drift velocity of particle considered

M = mass of particular particle considered

Because the time between collisions for electrons is much greater and their mass much less than either the positive or the negative ions, w_e will be very much greater than w_- or w_+. Therefore, it is assumed that the predominant current will be carried by electrons and the electron gain and loss processes will be the main processes considered in this report.

Ionization. Ionization is the process by which positive ions and free electrons are produced in a gas. There are really two types of gas discharges depending on the primary type of ionization used, the self-sustained and the externally sustained gas discharges. In the self-sustained discharge the ionization of gas molecules is caused primarily by the sustainer field (electric field) across the gas and the gas discharge will continue as long as the electric field is maintained. In the externally sustained gas discharge, an external source of electrons is used to cause ionization of the gas and allow the discharge to occur. For either case, when the rate of electron production through ionization drops below the rate of electron

14

loss through such processes as attachment and recombination, the gas discharge will cease. The externally sustained gas discharge is the one used in this study.

The external ionization source is commonly either ultra-violet radiation or an electron gun. The system in this study uses an electron gun. The electron gun fires a stream of electrons, emitted from an indirectly heated cathode and accelerated to an energy of 175 keV, through a thin titanium foil into the gas mixture. The high-energy electrons ionize the gas molecules generating a large number of secondary electrons. The secondary electrons have sufficient energy to ionize additional gas molecules and provide a high number density of low energy electrons and positive ions in the gas volume. The low energy electrons are then accelerated by the sustainer field and when sufficiently accelerated, can cause additional ionization of the gas. The types of reactions within a gas which create positive ions and free electrons as well as those which capture electrons and neutralize positive ions are portrayed in Table I.

In this application, the discharge is operated in a non-self-sustained mode; practically all ionization is supplied by the external e-beam. Therefore, the applied field-to-gas density ratio (E/N) is always lower than required for self-sustained operation. For the high pressures of the present system, a self-sustained discharge would immediately

15

TABLE I

Electron Kinetic Reactions [2:11]

Ionization

$A + e \longrightarrow A^+ + 2e$ ---Electron Impact

$A^* + e \longrightarrow A^+ + 2e$ --- Electron Impact

$A^* + B \longrightarrow A + B^+ + e$ --- Penning

Excitation

$A + e \longrightarrow A^* + e \longrightarrow A + e + hf$

Recombination

$A^+ + B + e \longrightarrow A + B$ --- Three-Body

$AB^+ + e \longrightarrow A + B$ --- Dissociative

$A^+ + e \longrightarrow A + hf$ --- Three-Body

Attachment

$AB + e \longrightarrow A^- + B$ --- Dissociative

$2A + e \longrightarrow A^- + A$ --- Three-Body

Detachment

$A^- + B \longrightarrow A + B + e$ --- Collisional

$A^- + hf \longrightarrow A + e$ --- Photo

$A^- + B \longrightarrow AB + e$ --- Associative
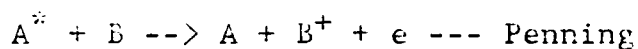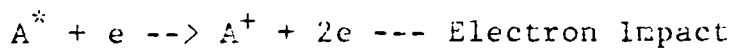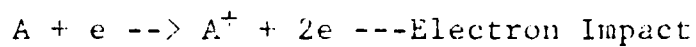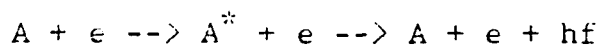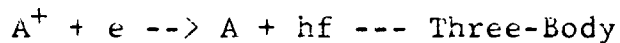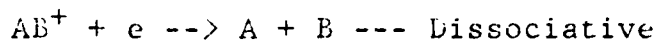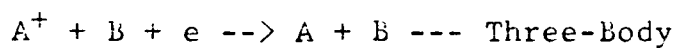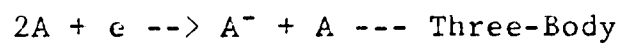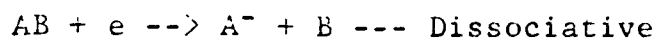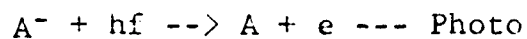
transition to an arc discharge and damage the device if the above condition were not met. However, the applied field and resulting E/N will determine other plasma parameters (drift velocity, recombination and attachment rates).

Recombination. Recombination is a particularly important de-ionization process at high pressures where electron and ion velocities are relatively slow. At constant temperature and pressure, the rate of recombination depends on the number of positive ions and negative ions or electrons present in the gas. For the present system, the number of positive ions is assumed equal to the number of electrons and negative ions, as stated earlier. Where the number of electrons is much larger than the number of negative ions, recombination is essentially a function of the square of the electron number density, n_e. Just as ionization was dependent on the value of E/N, so too is recombination. The attaching gas in the mixture considered here is a very small portion of the overall gas density (1/7550) and so is expected to play only a minor role in the recombination process. Therefore, the recombination rate is assumed to be the same as that for a pure methane gas, which has been calculated by Kline [3:19]. The recombination rate as a function of E/N presented in Figure 3 is the original rate predicted by Kline multiplied by a factor of 10 as suggested by Bletzinger [11:83] and later supported by Kline [12:230].

The recombination process in a gas discharge is usually in three forms as shown in Table I. As shown, the kinetic

17
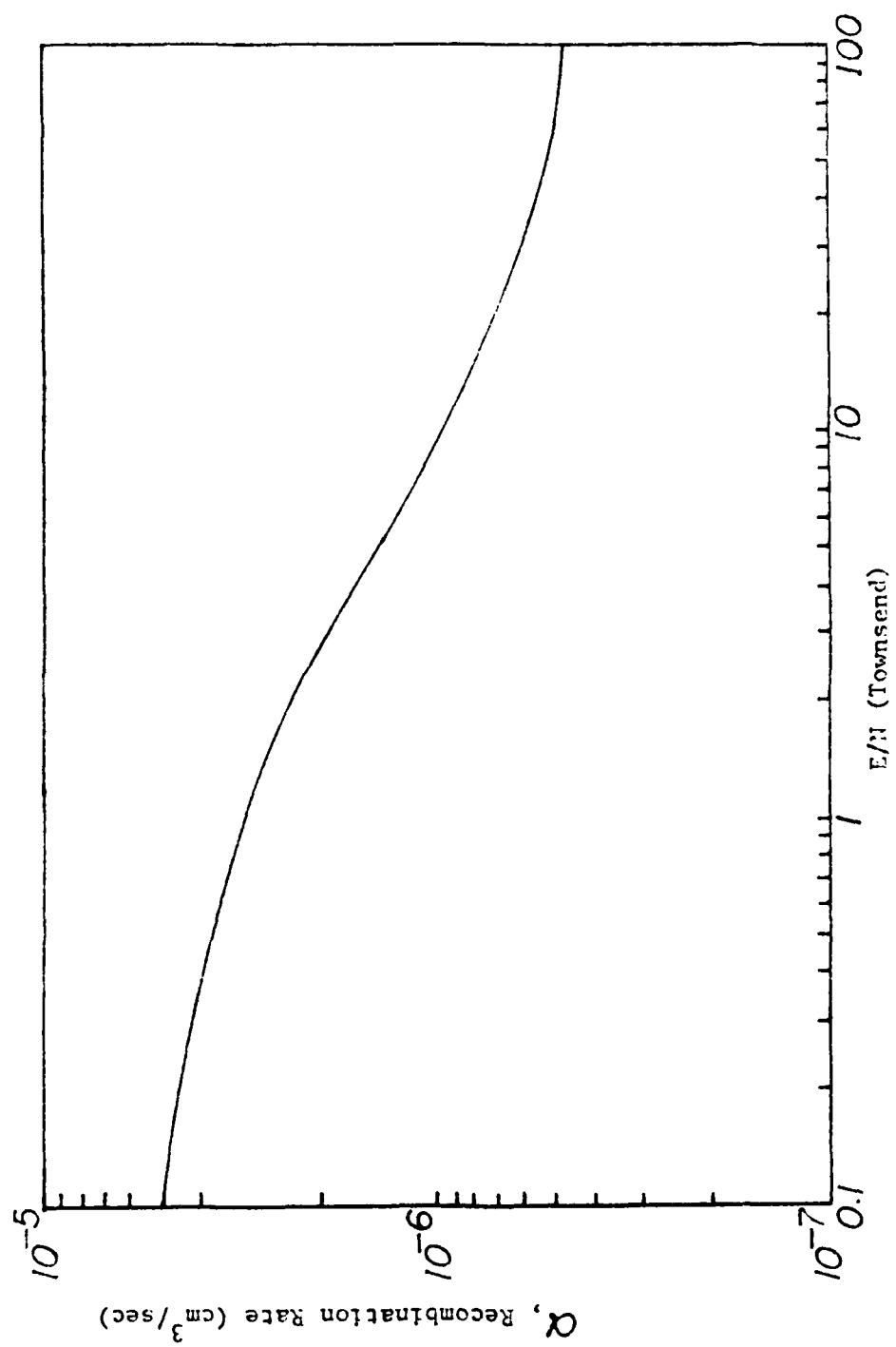
Figure 3. Recombination Rate vs E/N

and potential energy (of ionization) must be given either to radiation, as in radiative recombination, or to a third body, or to dissociation. The recombination processes have been presented in great detail in previous works [4:13-19, 11:83] and will be discussed further only when required to explain other processes more germane to this study.

Attachment. Frequently charged particles are assumed to be either positive ions or electrons. Indeed, for this study the predominant charged particles are assumed to be positive ions and electrons. However, in certain gases electrons can combine with neutral atoms, or molecules, to form negative ions and reduce the number of electrons in the discharge. Electronegative (attaching) gases exhibit this property. In such gases, the atoms have their outer electron shells nearly filled and thus have a high attraction for electrons. The perfluorocarbons are one of the groups of gases that are strongly electronegative. The perfluorocarbon, hexafluoroethane, is the subject of this investigation.

The process by which an electron, colliding with a neutral particle, forms a negative ion is called attachment. The attachment cross section for perfluoroethane is presented in Figure 4. Alternatively, the attachment rate coefficient, k_a, may be used, which is the fraction of attaching molecules that undergo attachment per sec with units of cm^3/sec. Christophorou measured the attachment rate of perfluoroethane and other perfluorocarbons in

19
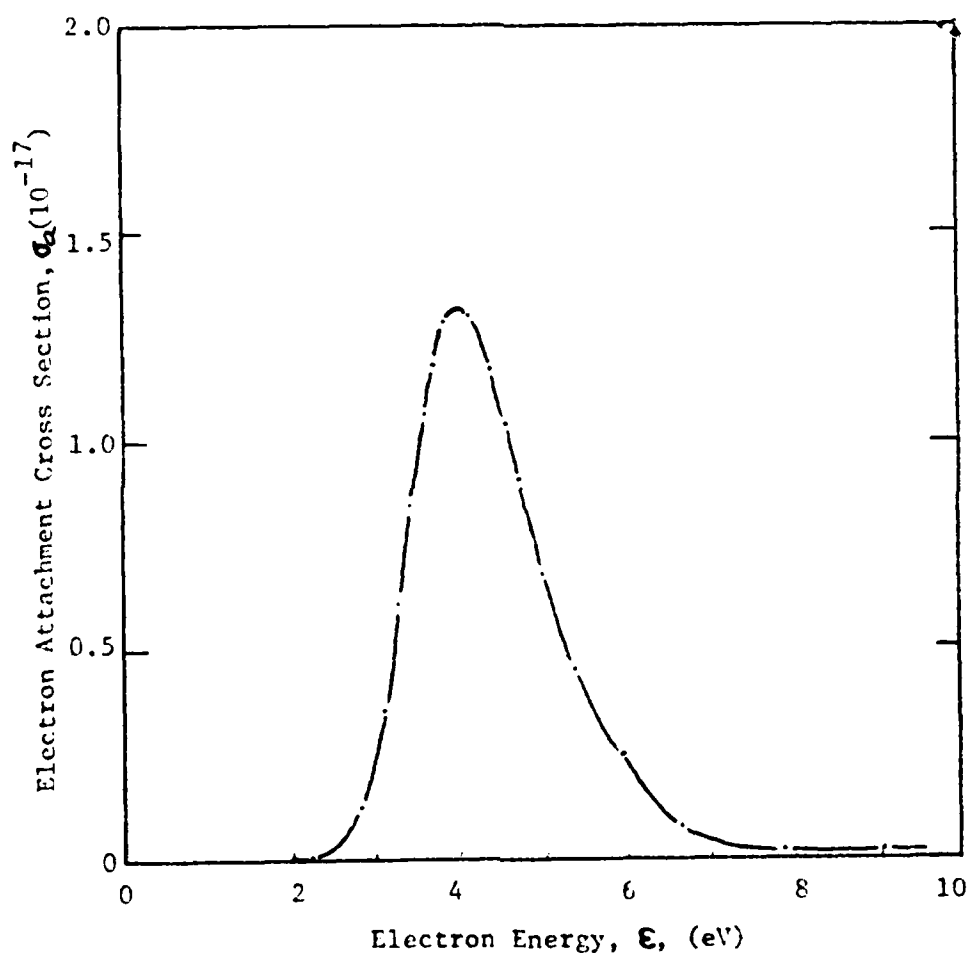
Figure 4. Attachment Cross Section for Perfluoroethane
[13:6155]

methane as a function of average electron energy using swarm studies [13:6155-6156]. However, his measurements didn't extend to lower average electron energies (below 1.2 eV for C_2F_6) and didn't use the large electron densities characteristic of e-beam switches, as is the intent of the current work.

The affinity for an electron by an electronegative particle is measured in electron volts (eV) and is normally on the order of 1 eV. This energy plus the kinetic energy of the electron must be dissipated during an attachment event. This may be done through radiation or, as shown in Table I, by giving both energy contributions immediately as kinetic energy to a third body or in the case of molecules, by dissociation. The two body dissociative attachment is the most probable attachment process for the present system where both the attachment rate and the dissociation rate of the electronegative gas are of interest.

III Theory

In this section the equations used to predict the performance of an e-beam controlled, diffuse gas discharge switch are described. The appropriate equations are solved, based on the assumptions presented in Section I, and the predicted results given. Also presented, are the theoretical calculations used to predict the dissociation rate of the attaching gas, C_2F_6, in a buffer gas of CH_4.

Plasma Modeling Equations

The transient and steady-state performance of an e-beam switch can be predicted provided certain reasonable assumptions are made concerning the properties of the plasma within the switch. The assumptions made in this study were presented in the first section of this report and further justified in Section II. The use of these assumptions considerably reduces the complexity of the equations used to describe the gas discharge. The three differential equations that model the change in electron and positive and negative ion densities within the plasma as a function of

time are [3:5]:

$$dn_e/dt = S - \alpha n_e n_+ - \beta n_e - \sigma \nabla^2 n_e + zn_e N \qquad (3.1)$$

$$dn_+/dt = S - \alpha n_e n_+ - k_i n_+ n_- + zn_e N \qquad (3.2)$$

$$dn_-/dt = \beta n_e - k_i n_+ n_- - D \qquad (3.3)$$

where

n_e, n_+, n_- = number density of electrons, positive and negative ions, respectively (cm^{-3})

t = time (sec)

S = electron beam electron-ion pair production rate (sec^{-1})

α = electron-ion recombination rate (cm^3/sec)

β = net attachment rate (sec^{-1}) ($= k_a n_a$, where k_a is the attachment coefficient and n_a is the number density of the attaching species)

σ = diffusion coefficient (cm^2/sec)

z = Townsend ionization coefficient (cm^{-1})

N = neutral gas number density (cm^{-3})

k_i = ion-ion recombination rate (cm^{-3}/sec)

D = Detachment term (included in attachment term during later analysis)

The assumption of spacial uniformity in the plasma implies that all important properties for this investigation apply uniformly throughout the bulk of the plasma. Further, since the electron current is assumed to dominate in the operating range of interest, the ionic currents will be omitted in the transient calculations. In fact, the negative ions will be neglected entirely in the steady-state

23

current analysis, except as products of dissociative attachment (negative ion current is predicted to be below the threshold current monitored in this report and should not effect the experimental results obtained). Also, the number density of electrons are assumed to equal that of positive ions $n_e = n_+$ (the major contribution to electrons and positive ions is due to the e-beam in the form of electron-positive-ion pairs). For the above reasons, Eq (3.1) will be used here to describe the characteristics of the plasma and will be expressed only in terms of electron charge carriers.

As discussed, diffusion losses will be neglected due to the high pressures and relatively large chamber dimensions involved. Also, for $0.1 < E/N < 20$ Td, the range studied by Duncan and Walker [14], electronic excitation, and ionization by the low energy (thermal) electrons (as opposed to the high-energy e-beam electrons) are negligible. This can be verified by the fact that the discharge is not self-sustaining, but instead rapidly decays upon removal of the e-beam current. These observations suggest that the terms due to diffusion and Townsend ionization can be dropped and since $n_e = n_+$, Eq (3.1) can be rewritten as

$$dn_e/dt = S - n_e^2 - n_e \qquad (3.4)$$

24

Setting the right side of Eq (3.4) equal to zero, the steady-state electron number density, n_{eo}, can be found to be

$$n_{eo} = [-\beta + (\beta^2 + 4\alpha S)^{1/2}]/2\alpha \qquad (3.5)$$

where S is evaluated using the relation

$$S = j_{eb}(Mm_p/eE_i)(dE/dm) \qquad [6:4822] \quad (3.6)$$

and where

j_{eb} = electron beam current (Amp cm^{-2})

M = mean molecular weight (g)

m_p = mass of a proton (1.67329 x 10^{-24}g)

E_i = effective ionization potential (Volts)

de/dm = mean stopping power of the gas (eV cm^2/g) [16:117]

Eq (3.4) can easily be integrated from e-beam turn-on (t= 0, n_e = 0) to t to give the temporal variation of n_e during turn-on

$$n_e = n_{eo}\left[\frac{(\beta +\alpha n_{eo})(Exp^{2\epsilon t} + 1)}{(\beta +\alpha n_{eo})(Exp^{2\epsilon t} + 1) - \beta}\right]\tanh \epsilon t \qquad (3.7)$$

where

$$\epsilon = n_{eo} + \beta/2$$

and again integrating Eq (3.4) from e-beam turn-off (t = 0,

25

$n_e = n_{eo}$) to t to get the temporal variation of n_e after e-beam turn-off

$$n_e = n_{eo}\beta/[(\alpha n_{eo} + \beta)\exp^{\beta t} - \alpha n_{eo}] \qquad (3.8)$$

The actual value of n_{eo} for a gas discharge can be computed from the practical equation

$$n_{eo} = I_d/(A_e W_e e) \qquad (3.9)$$

where

A_e = area of the current collector (cm^2)

W_e = drift velocity of electrons (cm/sec)

I_d = measured discharge current (Amps)

using the results of Eq (3.9) and computer techniques developed by Bletzinger [16], a least-squares fit of the decay portion of an actual discharge current pulse can be made to Eq (3.8). The results of the fit are the computed recombination and attachment rates for the gas mixture based on the actual discharge current decay curve (see Section V).

Dissociation Rate

There are two primary sources of attaching gas dissociation in this study. The first is the dissociation caused by high-energy primary and secondary electrons from the e-beam ionization source colliding with the neutral species. The second is caused by the bulk of low energy (thermal) electrons maintained by the sustainer field. Both sources of dissociation will be estimated based on available

data to establish an expected upper bound on the rate of attaching gas molecule dissociation.

E-beam Induced Dissociation. Ionization of the methane gas molecules as a result of the e-beam is approximately equal to the electron source term, S, which can be calculated using Eq (3.6). If it is assumed that the attaching gas molecules are ionized at only a slightly higher rate (scaled according to the partial pressure of the attaching gas) and that all ionization results in dissociation (worst case condition), then the rate of dissociation can be estimated to be

$$k_b = S(n_a/N) \tag{3.10}$$

where

  k_b = molecular dissociation rate due to the e-beam (cm^{-3} sec^{-1})

  n_a = number density of attaching species (cm^{-3})

  N = number density of all gas species (cm^{-3})

Thus, Eq (3.10) can be used to set an approximate upper bound on the rate of attaching gas molecular dissociation due directly to the e-beam ionization source. Some of the dissociated molecules will recombine at the high (>1 atm) pressures used in this study yielding an even lower rate of dissociation. However, for switching applications, only the net rate of dissociation and corresponding loss in electron attaching ability is of interest. Therefore, the net dissociation of the attaching gas on a macro scale will be

27

measured in this study.

Bulk (Sustainer Induced) Dissociation. The dissociation of attaching gas molecules resulting from electron-neutral species collisions with low energy (thermal) electrons that have been accelerated by the sustainer field can be calculated using the relation

$$k_d = n_a(2/m)^{1/2}\int_c^\infty f(\epsilon,E/N)\epsilon\,\sigma_d(\epsilon)\,d\epsilon \qquad (3.11)$$

where

$f(\epsilon,E/N)d$ = fraction of electrons in an energy range $d\epsilon$ about energy ϵ for a specific E/N normalized by dividing through by $\epsilon^{1/2}$

n_a = number density of attaching species (cm^{-3})

m = mass of an electron (9.11×10^{-28} g)

$\sigma_d(\epsilon)$ = total dissociation cross section of the attaching gas molecule (cm^2) [17:1425]

ϵ = electron energy (eV)

k_d = dissociation rate due to low energy discharge electrons ($cm_{-3}\ sec_{-1}$)

Since the gas mixture used here is over 99.98 per cent methane the electron distribution function as a function of E/N for the gas mixture will be essentially the same as that for methane. This distribution has been calculated using Boltzmann statistics and is presented in the next section for the maximum E/N possible in this study.

Cathode-Fall Voltage

The cathode-fall voltage is a function of e-beam current, discharge current, gas type and pressure, secondary

emission coefficient of the cathode material plus other less significant parameters [18]. Due to the complexity of the cathode-fall voltage calculations, the cathode-fall voltage will be experimentally determined using the method advanced by Bletzinger [5:38].

The e-beam controlled, gas discharge, on/off switch used in inductive storage pulsed power systems, must have a rapid switch-off time (< 1 μsec) and be capable of many (>10^5) operations to be competitive with other high-power switching systems [19:2-13]. The key to the operation of the switch is the gas mixture used in the discharge chamber. The goal of this experiment is to measure two of the properties desirable for the gas mixture used in the switch, electron attachment and dissociation rates of the attaching gas. This section will describe the equipment used as shown in Figure 5, the procedures and rationale used, and some of the problems encountered during the experiment.

Gas Mixture

The gas mixture used in the current system was 0.013 per cent perfluoroethane, C_2F_6, with the remainder being methane. The total pressure of the gas was maintained at atmospheric pressure to coincide with the desired operating pressure of systems which might use the switch.

Electron Gun

The present device uses an e-beam to ionize the gas between two electrodes in a closed cycle gas flow loop, thus, creating a plasma between the electrodes. An electric field, sustainer field, is established across the plasma by
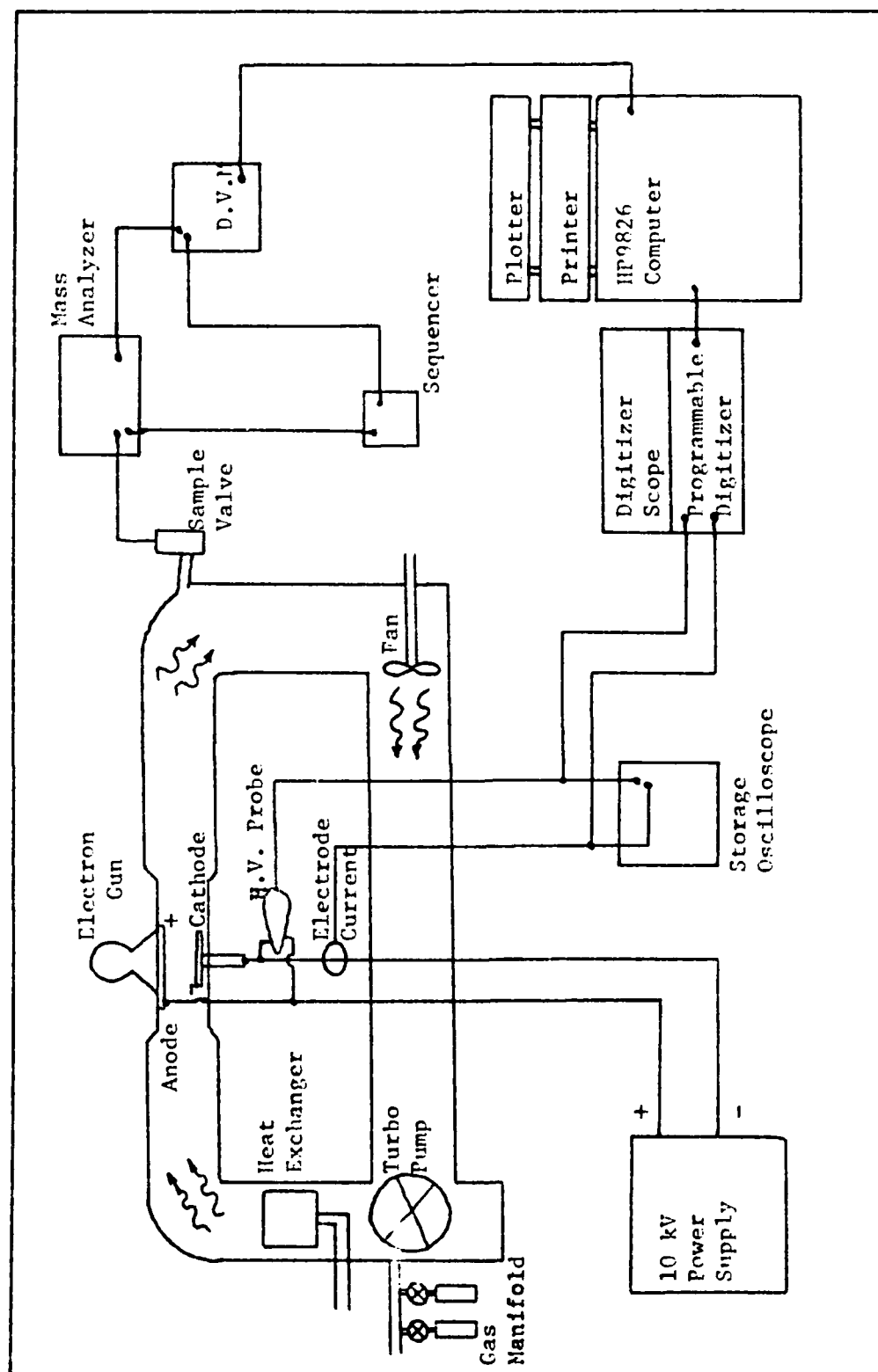
Figure 5. System Set-Up for Tests

placing a high-voltage potential difference on the electrodes. The sustainer field accelerates low energy electrons freed by the ionizing e-beam and causes some additional ionization, but mostly accounts for the bulk discharge current through the switch. The gas discharge is only maintained during the time the e-beam is on. Therefore, the system is said to be an e-beam sustained gas discharge switch. A system of this type has two controls on the gas discharge output (e-beam current and voltage and the sustainer field) and yields discharges that are scalable to large volumes at high-pressure.

The e-beam source used here is an Energy Sciences Inc. Model CBP 175/5/15 Electrocurtain electron gun. It is only slightly modified from that used in industry and is capable of CW or pulsed operation up to 1000 Hz and energies to 175 keV. In operation, electrons emitted from a low work function indirectly heated cathode are controlled and focussed by Pierce electrodes, accelerated by the gun potential (up to 175 kV) and passed through a titanium foil window into the target gas. The potential on the Pierce electrodes determines the e-beam current density, while the gun potential determines the energy of the electrons. The 0.5 mil titanium foil with dimensions of 5 cm by 15 cm acts as the window separating the target gas from the vacuum of the e-beam section and attenuates approximately 60 per cent of the e-beam current.

In the present configuration, the e-beam was operated

at 175 kV and from 100 mA to 1 A prefoil currents. Pulse rates were held below 5 pulses-per-sec (pps) and pulse widths (pw) below 70 usec during the investigation to minimize discharge heating effects. The rise and fall times of the e-beam pulse were typically less than .8 usec, (see Figure 6). However, after 4-5 hours of operation, the e-beam pulse would suddenly (over approximately 20 minutes time) change shape with the fall time increasing to 1.6 usec. This increase in fall time could not be tolerated since it directly effects the rate of decay of the discharge current. As will be seen later, the decay portion of the discharge current will be used to determine the electron attachment frequency of the gas. The e-beam pulse was monitored throughout the experiment to ensure that the desired pulse width, pulse shape, amplitude and frequency were maintained. Whenever any degradation in the pulse was observed, the experiment was temporarily stopped and the system allowed to stabilize before proceeding. Approximately 60-100 thousand pulses at 5 pps were possible before any system degradation occurred.

Discharge Chamber

The discharge chamber used in this experiment is the same as that used by Schneider [2:29-33], except that the electrode distance could be very accurately varied using a stepper motor driven micrometer from 0 to more than 3 cm.

33
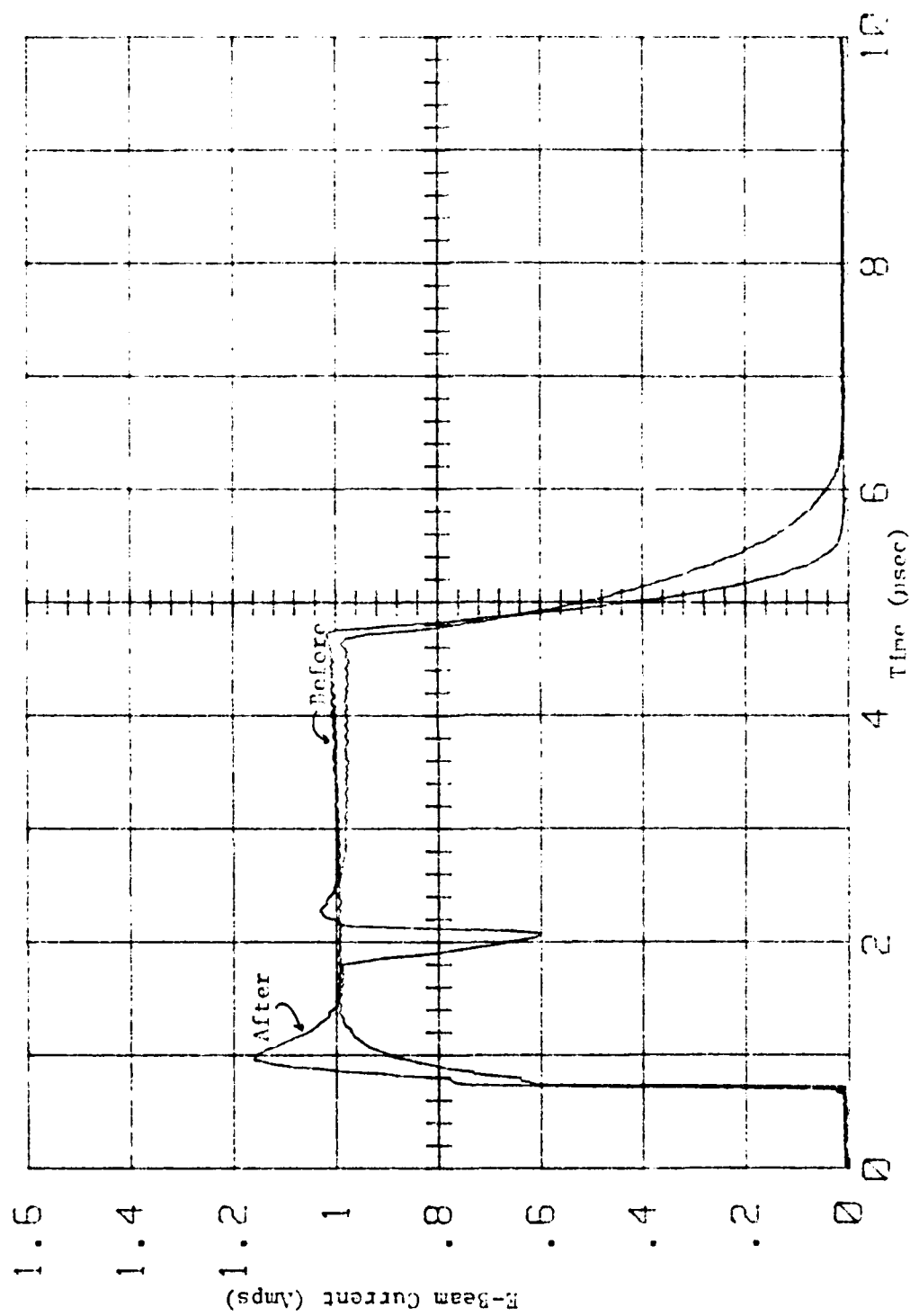
Figure 6. Typical E-Beam Pulses Before and After Operation for Long Period of Time

34

Figure 5. Typical E-Beam Pulses Before and After Operation for Long Period of Time

34

All experimental measurements were taken with the electrodes separated by 2.2 cm, except the cathode-fall measurements, which are discussed later.

Electrode Circuit. The cathode was biased negatively by a 10 kV power supply. The voltage across the sustainer field electrodes was supplied by a 1 μF, 30 kV capacitor in parallel with the electrodes. A current limited regulated power supply was used to charge the capacitor. This circuit allowed operation at the high E/N values required, while still providing arc discharge protection.

Closed-Cycle Gas Flow Loop

The closed-cycle gas flow loop is connected to the discharge chamber by bellows ducting and flanges with knife-edge seals at both inlet and outlet sections to prevent gas leaks. The loop is constructed of 15 cm diameter, high-vacuum, stainless steel ducts connected together by metal seal flanges. The total volume of the loop, computed to be 44.7 liters, was sealed off from the e-beam source by a thin titanium foil and was capable of pressures down to 10^{-9} torr. It was routinely pumped down to 10^{-8} torr during the course of this investigation to eliminate sources of gas contamination prior to infusion of the test gas.

Gas Evacuation and Filling. Evacuation of the loop was accomplished by two stages of pumps. The first pumping system was a large general purpose pump capable of pumping the system down to 10^{-4} torr on the external side of a

35

second pump. The second pump was a Leybold-Heraeus NT450 turbomolecular pump which evacuated the loop through an ultrahigh-vacuum valve down to the 10^{-8} torr range. The process of evacuating the loop required approximately 48-72 hours, but was necessary to prevent the possibility of contaminants in the flow loop.

Initial attempts to fill and maintain the pressure in the flow loop at atmospheric pressure were unsuccessful due to a system leak. Through system analysis it was decided that the gas was escaping through a large bellows valve between the flow loop and the evacuation pumps. To alleviate the problem, the following steps were taken in filling and operating the system for each new gas:

1. The valves were opened to the vacuum system and the loop evacuated to the 10^{-7} torr range or below.

2. The valves were closed and the system filled with the attaching gas to the desired partial pressure.

3. The Buffer gas was added to bring the total pressure up to the desired operating range.

4. The vacuum system was turned-off and the vacuum lines between the loop and the vacuum pumps isolated.

5. The vacuum line between the vacuum pump and loop was filled with nitrogen to the same pressure as the flow loop.

Using the steps outlined above, the pressure in the loop was easily maintained within 5 torr of the desire operating pressure for the entire experiment. Only gas of the highest purity was used, e.g., 99.97%-CH_4, 99.7%-C_2F_6. Also,

extreme care was taken to ensure no contaminants were allowed to enter through the inlet manifold.

Cooling and Circulation. The loop was cooled by a 1 kW heat exchanger to remove the waste heat from the discharge. A variable speed axial fan circulated the gas through the loop at flow speeds up to 10 m/s. The fan was externally driven with the drive mechanics sealed from the loop by a ferrofluidic rotary seal.

Mass Analysis

Mass analysis of the test gas was performed using an Inticon IQ-200 mass analyzer. It was hoped that the dissociation rate of the attaching gas and the molecular species present in the gas could be measured using this device. However, the extreme sensitivity ($>10^{12}$ for the amplifier gain and near maximum electron multiplier voltage) required to detect the attaching gas dissociation products were near the limits of the device. Therefore, large fluctuations in the amplitude of the measured data were experienced. The ions associated with the attaching gas were observed and identified, but the mass analyzer could not be used to determine the small dissociation rate expected in this study.

The mass analyzer input valve was located approximately 1 meter down stream from the discharge chamber. Gas was allowed into the mass analyzer's sample reservoir in minute amounts through an ultra-high vacuum, electrically control-

37

led valve. Prior to sampling the gas from the loop, the mass analyzer sample chamber was evacuated down to the 10^{-8} torr range through another electrically controlled, ultra-high vacuum valve using a Leybold-Heraeus turbomolecular pump. The gas pressure in the sample chamber could be precisely set at the same pressure (approximately 10^{-6} torr) for each gas measurement taken, to ensure repeatability.

Two methods were used to extract the mass analyzer data. The first method used a table output mode available on the analyzer to monitor a maximum of 10 different atomic masses (a complete description of the operation of the mass analyzer and available outputs is available in the equipment's operating manual) [21]. Up to 100 measurements were taken for each gas sample and the table outputs recorded using a digital computer. The 100 measurements were then averaged for each atomic mass and a standard deviation computed. This procedure was repeated at the beginning and end of each pulsing session for a total of 300,000 pulses of the e-beam.

The second method of extracting mass analyzer data was to digitize the X-Y plotter output from the analyzer using a Hewlett-Packard model 3478A digital multimeter. The mass analyzer was set on analog mode and allowed a range of 0 to 200 atomic mass units to be viewed at one time. The analog signals from the analyzer were transformed into digital signals by the digital multimeter and recorded using the Hewlett-Packard 9826 computer. The mass analyzer analog outputs stored on the 9826 computer are shown in Appendix C.

38

Diagnostics and Data Reduction

As discussed, two processes were monitored in this investigation, electron attachment and molecular dissociation of the attaching gas. The electron attachment rate was measured by monitoring and digitizing the discharge current pulse, then using a computer to perform a least-squares fit of the decay portion of the pulse to Eq (3.8). The second process, that of molecular dissociation, also used the change in attachment rate to indicate the amount of dissociation that had occurred. Additionally, an unsuccessful attempt was made to measure the rate of molecular dissociation through mass analysis. However, the errors associated with the mass analysis technique prevented use of the data in determining the relative dissociation of the attaching gas.

Attachment Rate. The discharge current used to determine the attachment rate was measured using a Pearson Pulse Transformer Model 411 with a sensitivity of 0.1 V/A. The transformer coil was positioned around the high voltage cable from the 1 μF capacitor to the electrode and monitored all of the discharge current passing through the electrode. The discharge voltage was determined using a high voltage probe. Both signals could be input to a Tektronix model 468 storage oscilloscope or to a Tektronix model 7912AD programmable digitizer via standard Rf cables and connectors. The accuracy of these devices are listed in Appendix A.

The storage oscilloscope was used throughout the experiment for real time monitoring of system parameters, i.e., e-beam current pulse, discharge current pulse, and/or the discharge voltage. This was necessary to ensure that all parameters were stabilized and accurate prior to sampling a desired system output. The storage capability was particularly important to ensure that the e-beam pulse had not changed during the experiment, as mentioned earlier. By using the storage capability, the e-beam pulse could be continually compared with one taken at the beginning of a measurement session and any discrepancies quickly identified.

The test data was sent to the programmable digitizer where it was displayed and digitized for input to a Hewlett-Packard 9826 computer. The digitizer provided up to 512 storage locations, or bins, each representing the amplitude of the signal as a function of the horizontal distance across the digitizer's scope trace. The digitized data sent to the computer was stored on magnetic discs for later analysis. The software used in the computer to extract, store, and analyze the digitized data was developed for similar experiments by Bletzinger [16].

The process of digitizing and recording the data on magnetic discs for later analysis was a highly efficient and accurate way of retrieving the measured data. Not only could more experimental time be spent monitoring and adjusting system operating parameters, but much more flexibility

was allowed in analyzing the data. Using the computer the data could be scaled, offset, overlayed with theoretical or other measured data, shifted, normalized, and/or its value accurately determined at any point. Also, the computer was used to calculate the cathode-fall, compute n_{eo} from the steady state discharge current, fit the decay portion of the discharge current to Eq (3.8), and compute the attachment and recombination rates based upon the fit.

The curve fitting procedure mentioned previously to calculate the attachment rate from the decay portion of the discharge current pulse is not a new procedure [2:34-40,16]. Schneider demonstrated that errors of less than 10% can be expected if a sufficiently long portion of the decay curve is used [2:39-40]. To achieve this accuracy Schneider used a ratio of initial (n_{eo}) to final (n_f) electron number densities of at least 100 which was independent of time. This was the criteria used in this study, except that the first usec of decay was not used in the curve fit procedure. In eliminating the first usec of the decay curve, the major source of error, that due to the slow e-beam decay, was minimized (note: e-beam decay was approximately .8 μsec). Since the initial portion of the current decay curve is expected to be recombination dominated, little is lost by eliminating this portion of the curve in determining the attachment rate. Figure 7 is a plot of the decay portion of a representative discharge current pulse overlayed by a plot of Eq (3.8) using values for α, β, and n_{eo} determined by

41

Electron Number Density, n_e (cm^{-3})

1.1E+12

8.6E+11

6.4E+11

4.3E+11

2.1E+11

0.0E+00

3.3E-08 2.5E-06 2.5E-06 3.0E-06 2.4E-06 9.9E-06 1.2E-05

Time (μsec)
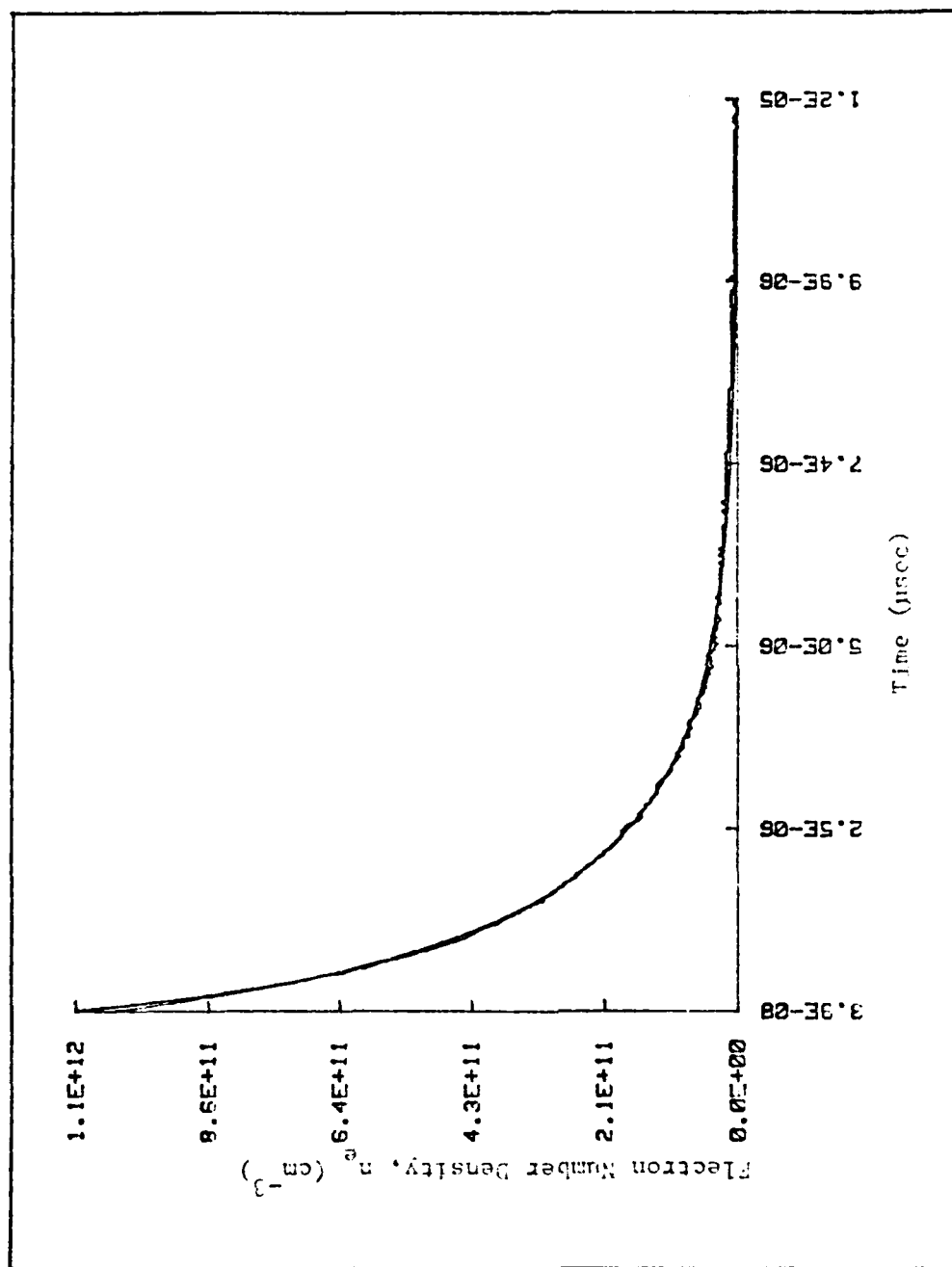
Figure 7. Typical Plot of Current Decay and Computer Fit

42

the fitting routine. Using the procedure just described the uncertainty in attachment rate is expected to be less than 5%.

Molecular Dissociation. The dissociation of C_2F_6 for this experiment was expected to be less than 0.1%. This was based on theoretical calculations as outlined in Section III using the gas ionization rate, electron energy distribution of CH_4, and the dissociation cross section of C_2F_6. The mass analyzer was insensitive to such small changes in the amount of attaching gas present in the gas mixture. This was due to the the extremely small fraction of attaching gas in the mixture(.013%) which caused the standard deviation in the output of the mass analyzer to be on the order of 80% of the mass reading. Therefore, the change in attachment rate as a function of discharge current, e-beam current, and total discharge time was used to gain some knowledge of the rate of dissociation. This method assumes that the products of dissociation are not highly electronegative. However in reality gas products from dissociation, such as fluorine, may account for a significant portion of the electron attachment and cause the measured rate of dissociation to be much lower than it actually is.

Another method, not performed here, which may be used to measure changes in the gas mixture composition, is laser spectrometry. This method was not used due to non-availability of equipment, and the complexity of the method. Also, the low rate of dissociation indicated in theory and

43

substantiated by the lack of change in attachment rate, suggests that dissociation of C_2F_6 is not a critical factor in the design of an e-beam switch with relatively large circulating gas volumes.

Cathode-Fall Voltage. The cathode-fall voltage was determined by establishing a discharge current for a specific combination of e-beam current and voltage, electrode potential difference and separation, and gas mixture. Then the separation was changed while adjusting the electrode potential to maintain constant discharge current. In this manner the moving electrode was used as a voltage probe and constant E/N was roughly maintained through constant discharge current. A series of five measurements of the discharge voltage corresponding to different electrode separations were made for each combinations of E/N and e-beam current. A linear least-squares fit to the five measurements of discharge voltage was made and extrapolated to zero electrode separation using the 9326 computer to yield the cathode-fall voltage.

V Results and Analysis

In Figures (8) and (9) are shown predicted discharge current decay curves using Eq (3.8) with n_{eo} equal to 1.6 x 10^{12} cm^{-3}. The value of n_{eo} was derived from the measured current density and the known drift velocity at a measured E/N and is characteristic of this experiment. The value of n_{eo} used was also computed using Eq (3.5) of Section III. This computed value of n_{eo} was within 20% of that derived from the measured current during the experiment. In Figure (8) recombination is held constant and attachment is varied; in Figure (9) attachment is held constant and recombination is varied. The effects of the recombination and attachment rates and the regions where they have their most pronounced effect is quite evident. A recombination rate of 8 x 10^{-7} cm^{-3} sec^{-1} was expected based upon the discussion in Section II. Also, attachment frequencies of 10^4-10^5 sec^{-1} were expected based upon swarm data by Christophorou [13:6155-6156] and e-beam experiments by Bletzinger [16].

The dissociation of C_2F_6 was first estimated by assuming a Maxwell-Boltzmann electron energy distribution (Figure 10) folded with the dissociation cross section from Winters [17:26] (Figure 11). The resulting dissociation rate as a function of mean electron temperature (eV) is shown in Figure 12. Even at a mean electron temperature of 1.5 eV, the dissociation rate is less than 5 x 10^{16} sec^{-1}. Thus, less than 2% of the total attaching gas available in the

45

SS Electron Number Density, n_{eo}	Recombination Rate α	Attachment Rate β	Source Term S
1.6×10^{12}	8×10^7	1.00×10^5	2.2×10^{19}
1.6×10^{12}	9×10^7	1.83×10^5	2.3×10^{19}
1.6×10^{12}	8×10^7	2.70×10^5	2.5×10^{19}
1.6×10^{12}	8×10^7	3.50×10^5	2.6×10^{19}
1.6×10^{12}	8×10^7	4.33×10^5	2.7×10^{19}
1.6×10^{12}	8×10^7	5.17×10^5	2.9×10^{19}

Increasing Attachment

TIME (μsec)

N_e (cm-3)

1.6E+12

1.3E+12

9.6E+11

6.4E+11

3.2E+11

0.0E+00

0.0   2.0   4.0   6.0   8.0   10.0   12.0
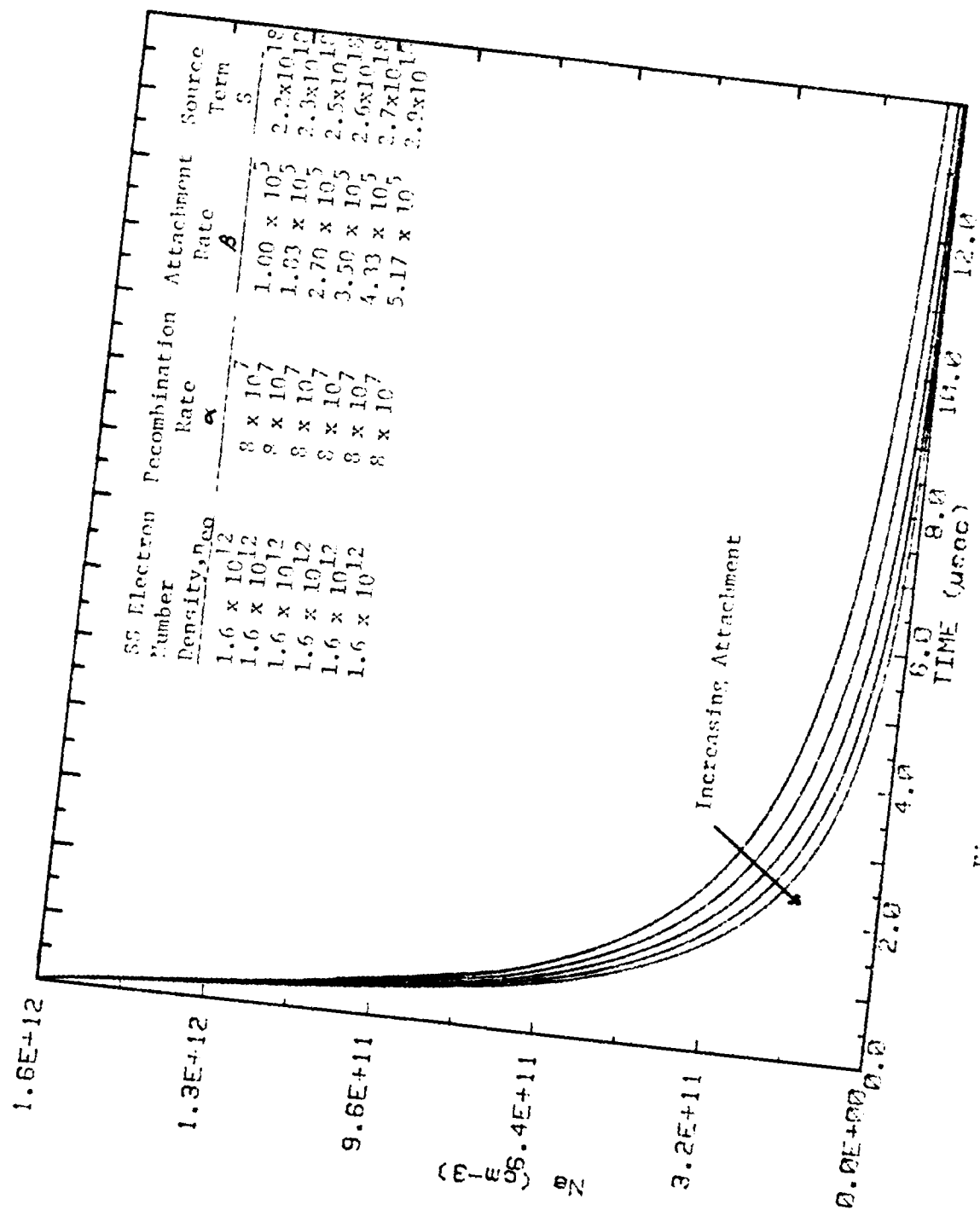
Figure 8. Predicted Current Decay--Varying Attachment.

46

SS Electron Number Density ($\times 10^{12}$)	Recombination Rate α ($\times 10^7$)	Attachment Rate β ($\times 10^5$)	Source Term S ($\times 10^{12}$)
1.6	2.00	5.00	1.31
1.6	3.33	5.00	1.65
1.6	4.67	5.00	1.99
1.6	6.00	5.00	2.34
1.6	7.33	5.00	2.68
1.6	8.67	5.00	3.02

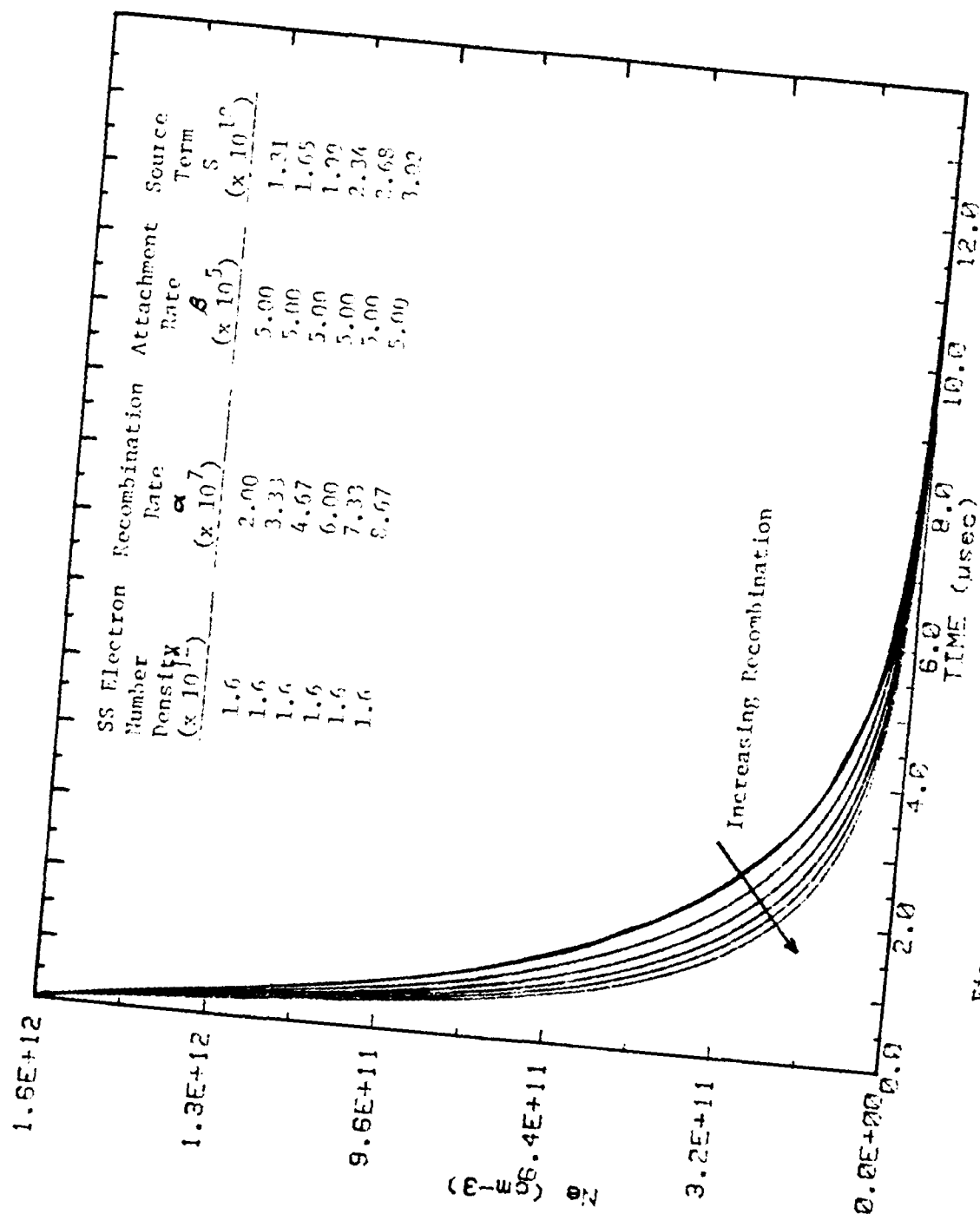Increasing Recombination

Ne (cm-3)

TIME (μsec)

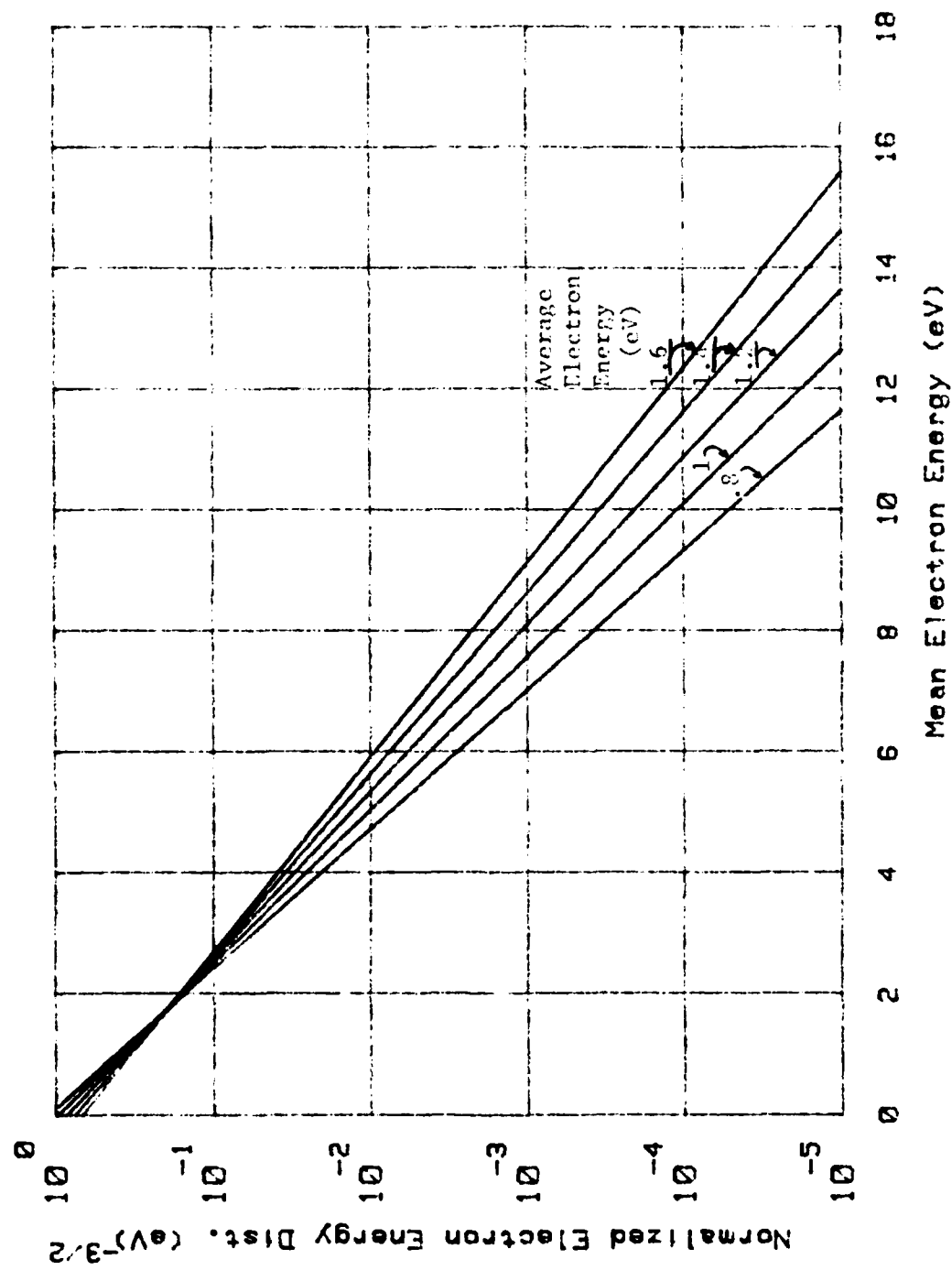Figure 2. Predicted Current Decay—Recombination Varying;

47

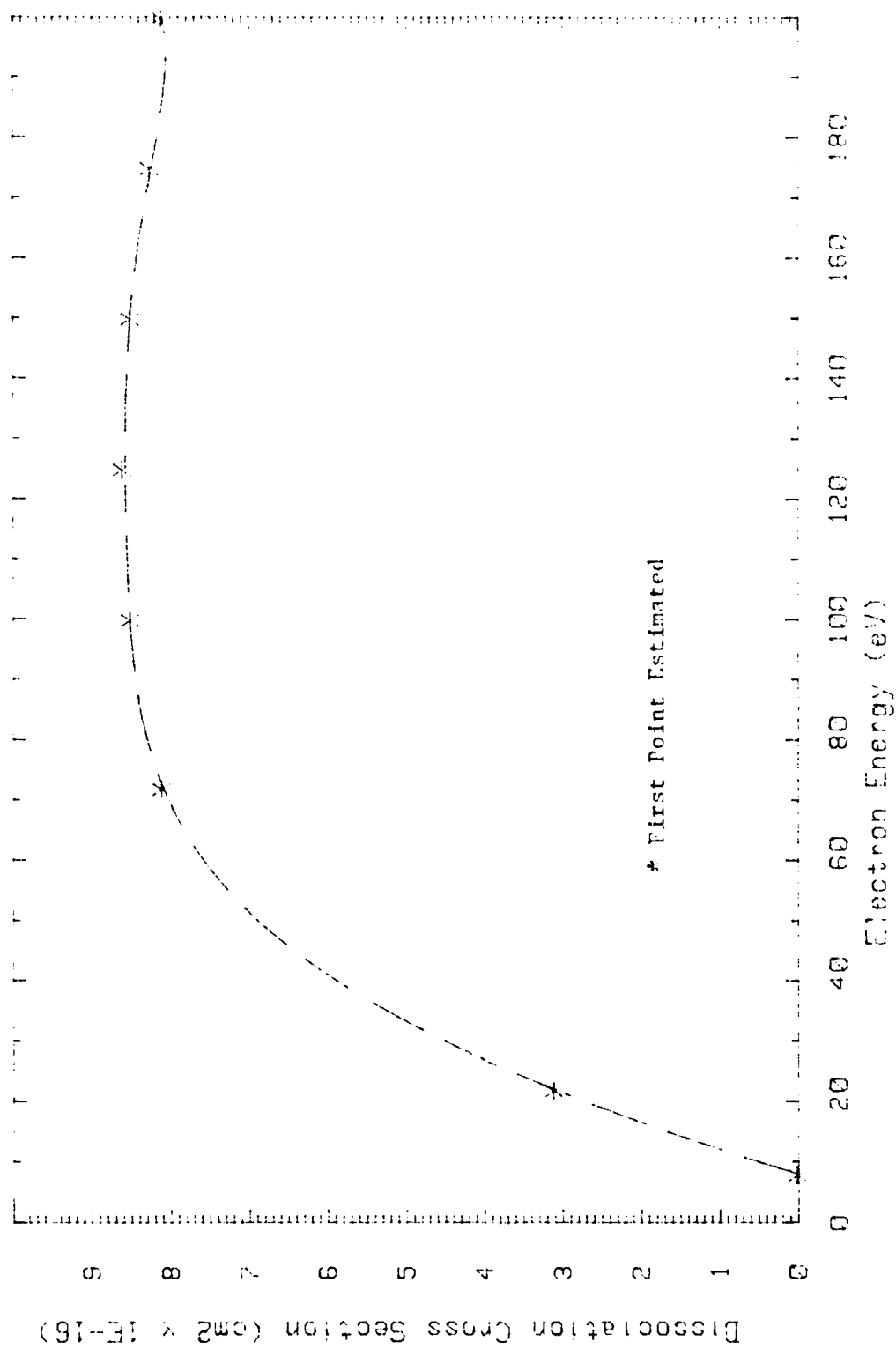Figure 10. Maxwell-Boltzmann Energy Distribution

48

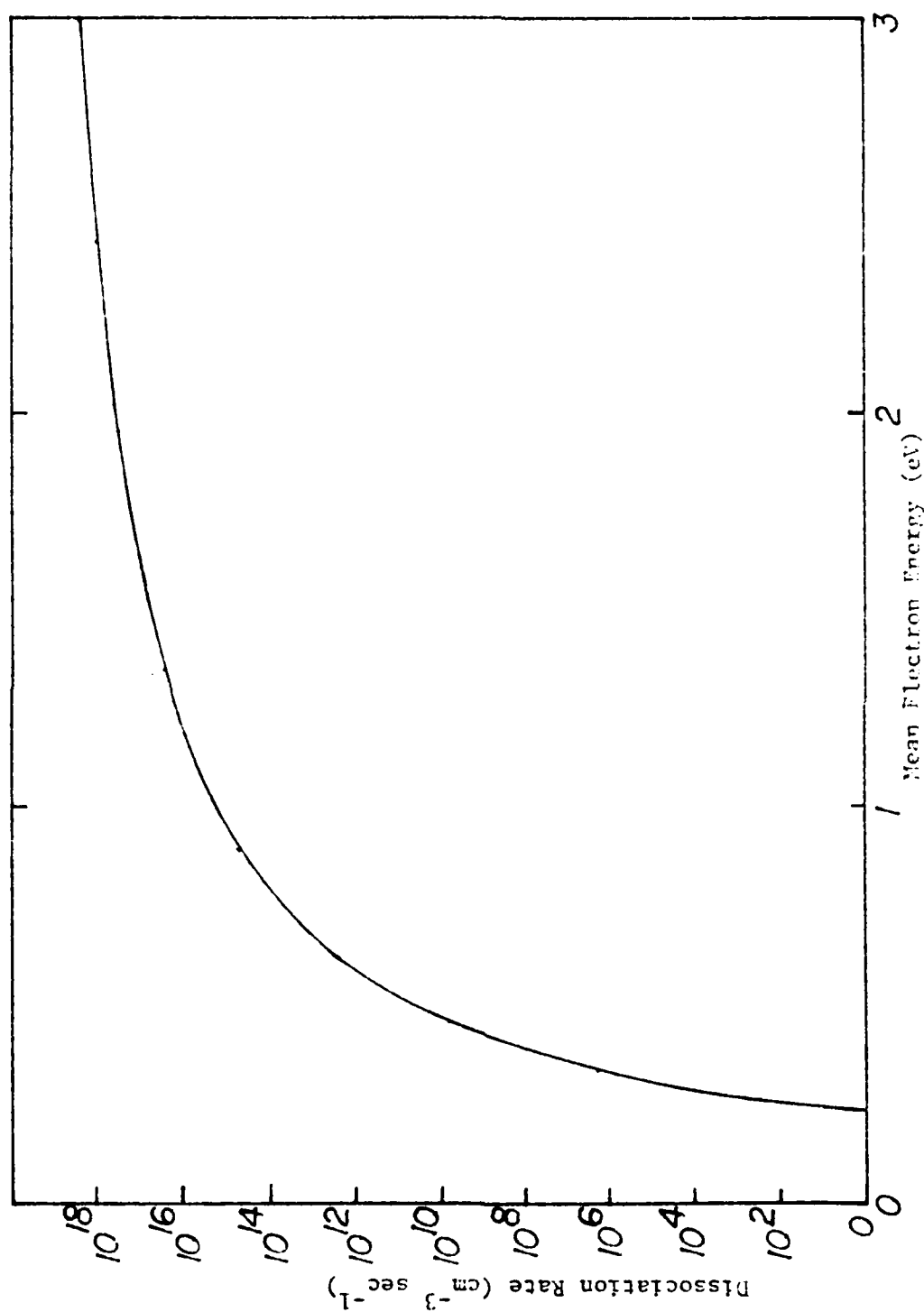Figure 11. Dissociation Cross Section for C_2F_6 [17:26]

Figure 12. Predicted Dissociation Rate Based on Boltzmann Distribution for C_2F_6

flow loop was expected to dissociated after 300,000, 4-µsec long, gas discharges (note: At the maximum E/N the mean electron temperature was less than 1.2 eV).

A later Boltzmann transport equation calculation of the actual, non-Boltzmann, distribution of electron energies using methane cross sections (Figure 13) indicated a significant decrease (several orders of magnitude) in the number of electrons at higher energies able to cause dissociation. Therefore, it was determined that the major contribution to dissociation of the attaching gas molecules is from the high energy e-beam electrons. Using the rational of Section III and Eq (3.10), the attaching gas dissociation rate was predicted to be less than 10^{15} cm^{-3} sec^{-1} in the discharge chamber. The total volume of the gas flow loop was 44.7 liters and that of the discharge chamber alone, 0.165 liters. Therefore, the percentage of C_2F_6 expected to dissociate per sec of discharge was less than 0.05% sec^{-1} or less than 0.06% for 300,000, 4-µsec wide pulses, at the maximum operating conditions of this experiment.

Cathode-Fall Measurements

The fill gas used to determine the cathode-fall measurements was 700 torr of 1/7550, C_2F_6/CH_4 gas mixture. Oscillations on the discharge current pulse (see Figure 14) made constant E/N adjustments very difficult for E/N greater than 3 T_d. Therefore, to obtain the most accurate cathode-fall voltage possible, several measurements were made at
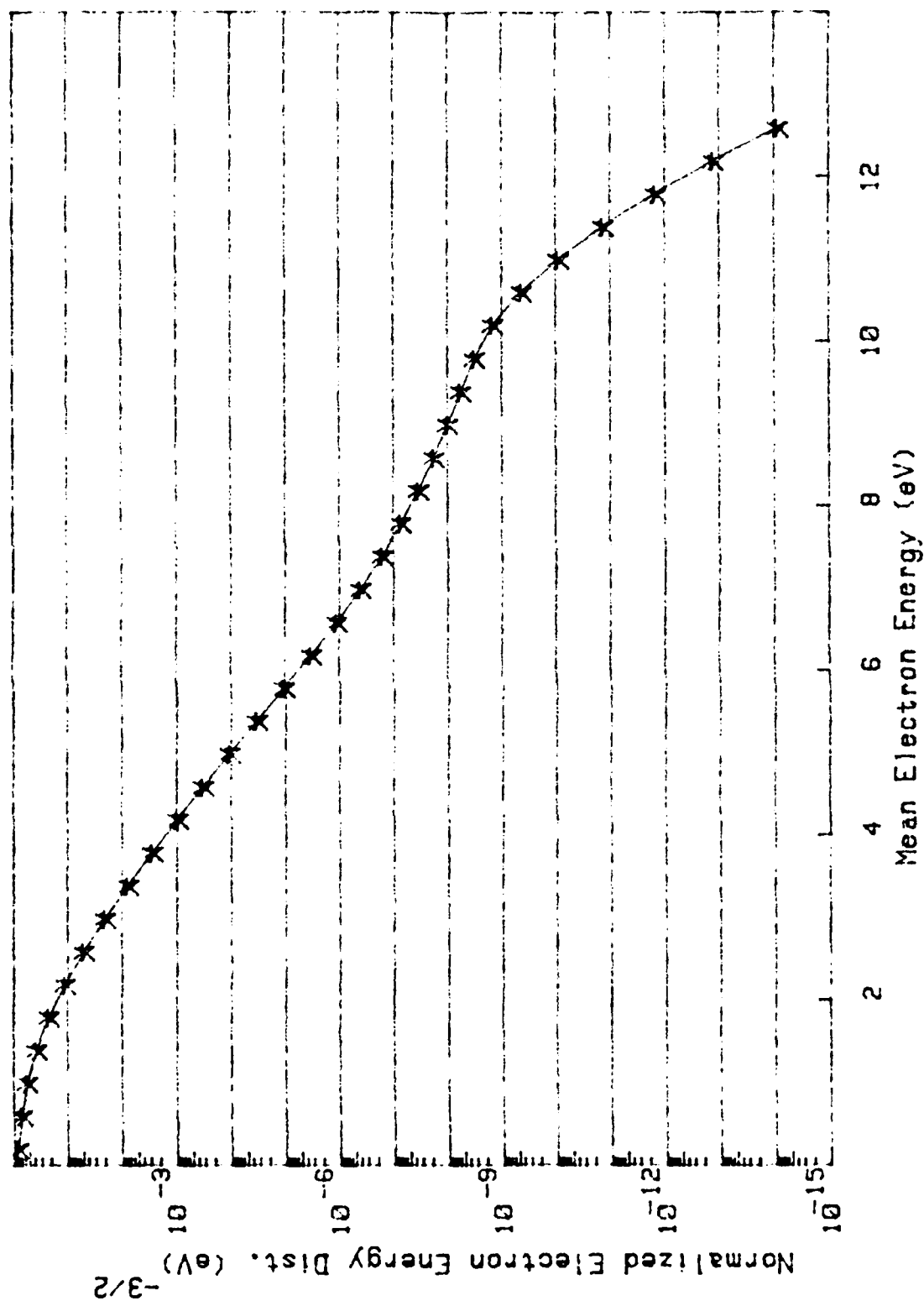
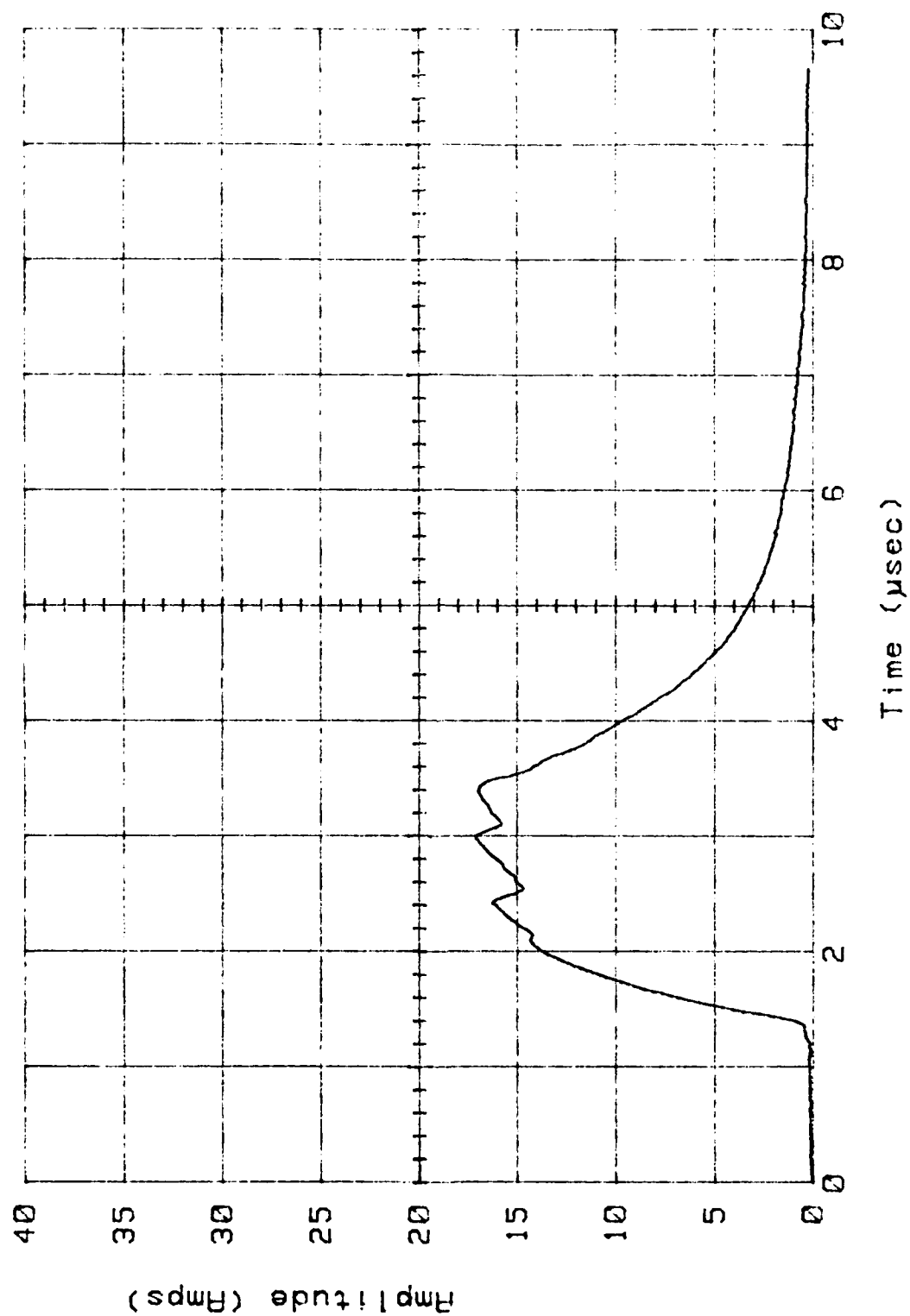Figure 13. Non-Boltzmann Energy Distribution In Methane

Figure 14. Discharge Current Pulse with Oscillations

each electrode separation, e-beam current and electrode voltage used. Then the results were averaged, plotted and fit to a mathematical equation using the computer and the method of least-squares. The cathode-fall voltage vs discharge voltage is shown in Figure 15 for e-beam currents of 400 mA and 1 A and over the range of discharge voltage from 0 to 9 kV. It was difficult to determine the exact uncertainty for the cathode-fall measurements; however, the values shown are expected to be certain to within 20%.

Measurements in CH_4

Experiments using 700 torr of pure CH_4 were conducted to obtain a baseline for comparison with the proposed gas mixture in this study. Table VI, in Appendix C, lists the atomic mass units (amu) observed using the residual gas analyzer for pure CH_4. Although some water vapor was also observed, it was not listed in the table. Tables II and III, Appendix B, list the properties of CH_4 during e-beam operation with e-beam prefoil currents at 400 mA and 1 A and with 13 different discharge voltages spanning the range of the electrode power supply.

A plot of the typical discharge current pulse is shown in Figure 16 where it is observed that the discharge current effectively falls to zero within 30 µsec after e-beam turn-off. It is also seen in Figure 16, that the transition between current rise and fall is not abrupt as expected from Eq (3.8), but instead tends to change slowly during the
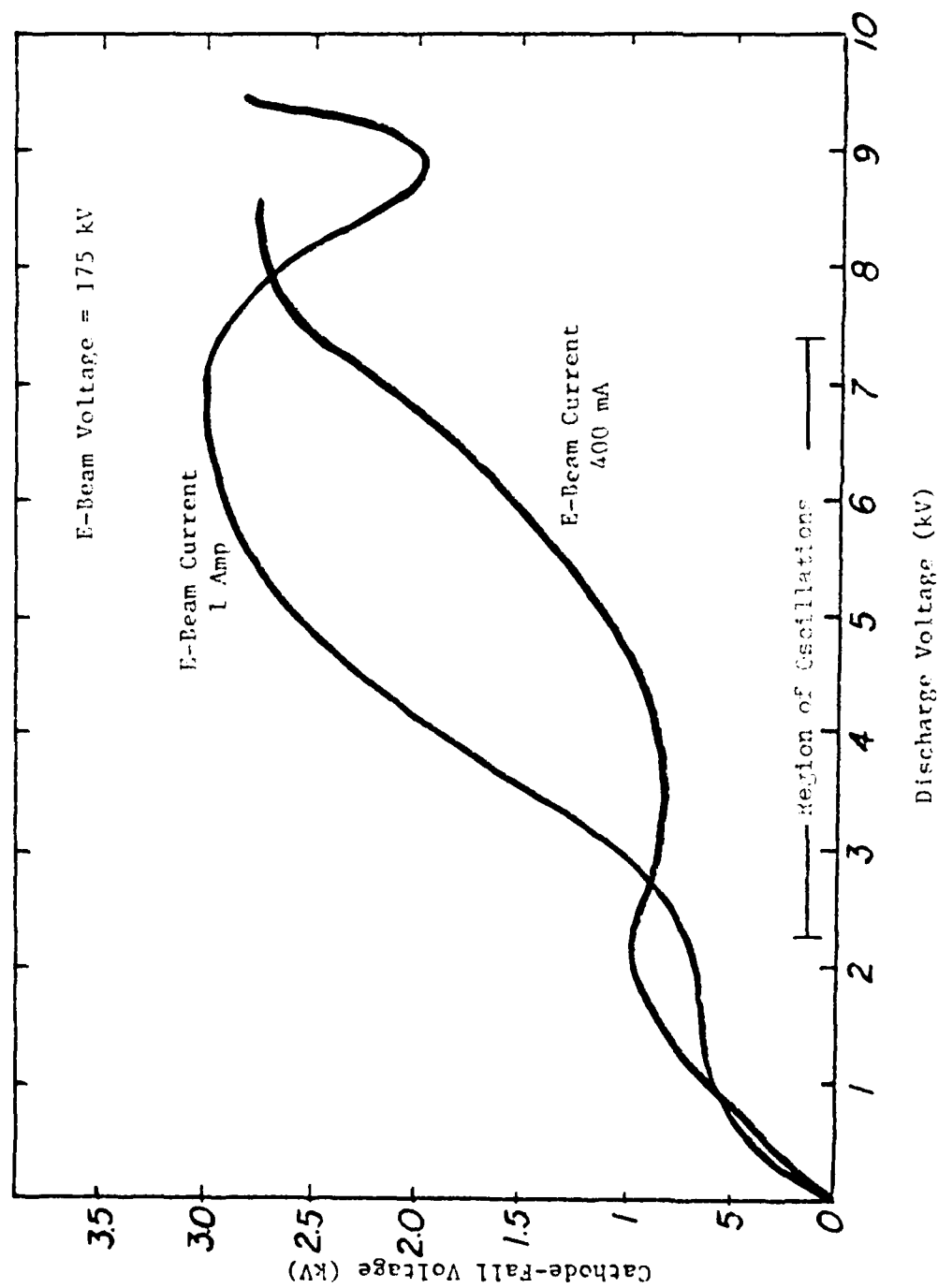
Figure 15. Cathode-Fall vs Discharge Voltage
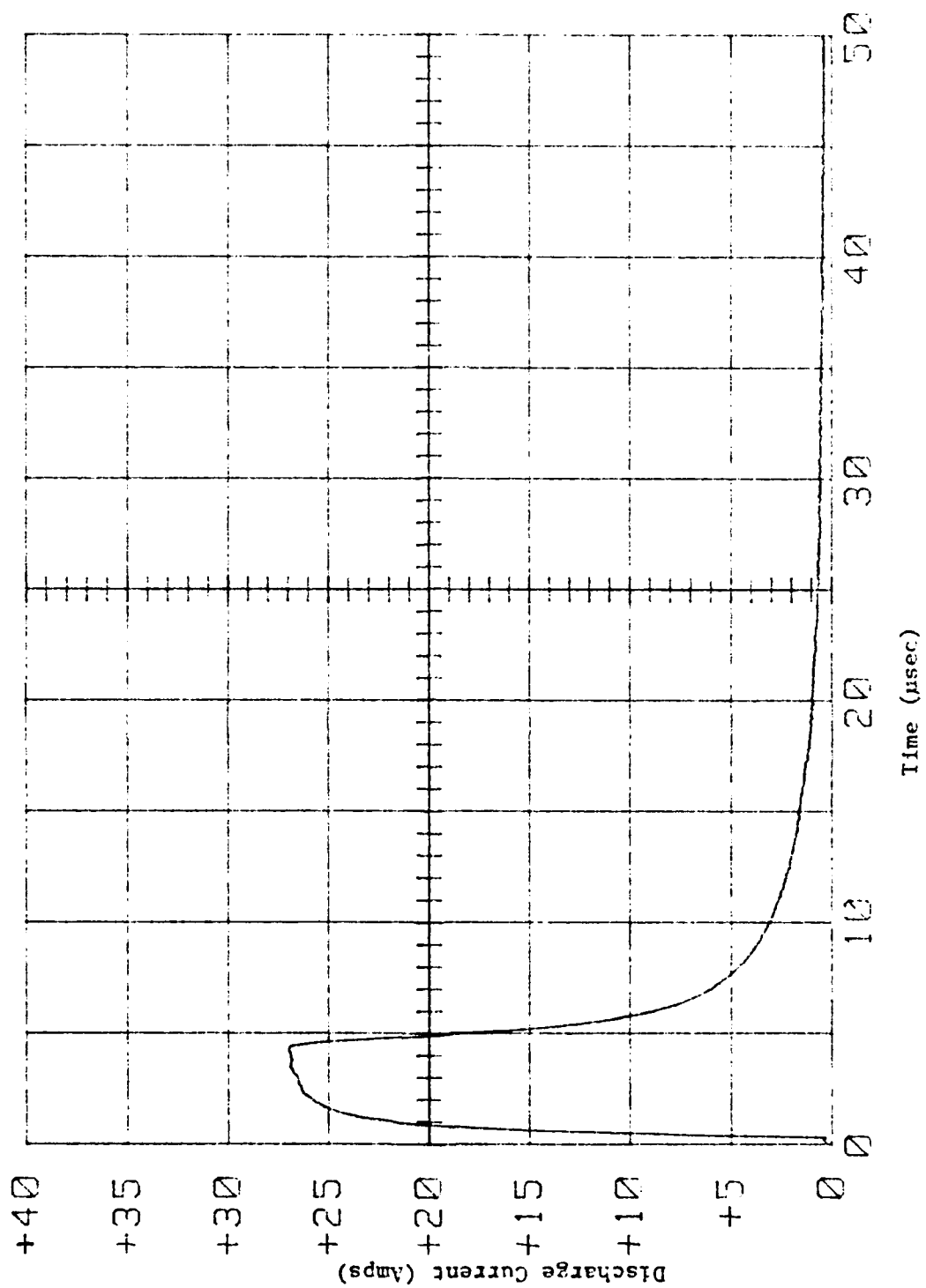
Figure 16. Typical CH_4 Discharge Current Pulse

first 0.1 µsec after e-beam turn-off. This slow transition between rise and fall is most likely due to the slow decay in the ionizing e-beam pulse as was evident in Figure 6. At low E/N ($<$ 3 T_d) the e-beam current contribution to the total discharge current is significant. Attempts to fit the total curve to Eq (3.8) in this region yields inconclusive results with α much lower than expected (negative at very low E/N) and β much higher than anticipated. This appears to have been the problem experienced in the earlier e-beam studies by Schneider [2:44-50]. At higher E/N ($>$ 3 T_d) the slow e-beam decay is less significant and recombination rates in good agreement with published literature were obtained [3:19,12:230]. The good agreement for recombination rates indicates that the rates computed for attachment should also be reliable.

In this study, the accuracy of the fitting procedure in obtaining the attachment rate was increased by eliminating the first µsec of the decay curve before fitting it to Eq (3.8). Figure 17 is a typical plot of the decay portion of a discharge current pulse where the initial portion of the decay has been ignored and the least-squares fit applied to the remaining portion of the curve. Eq (3.8) is plotted over the actual decay curve in Figure 17 using the results of the fitting routine for α, β, and n_{eo}.
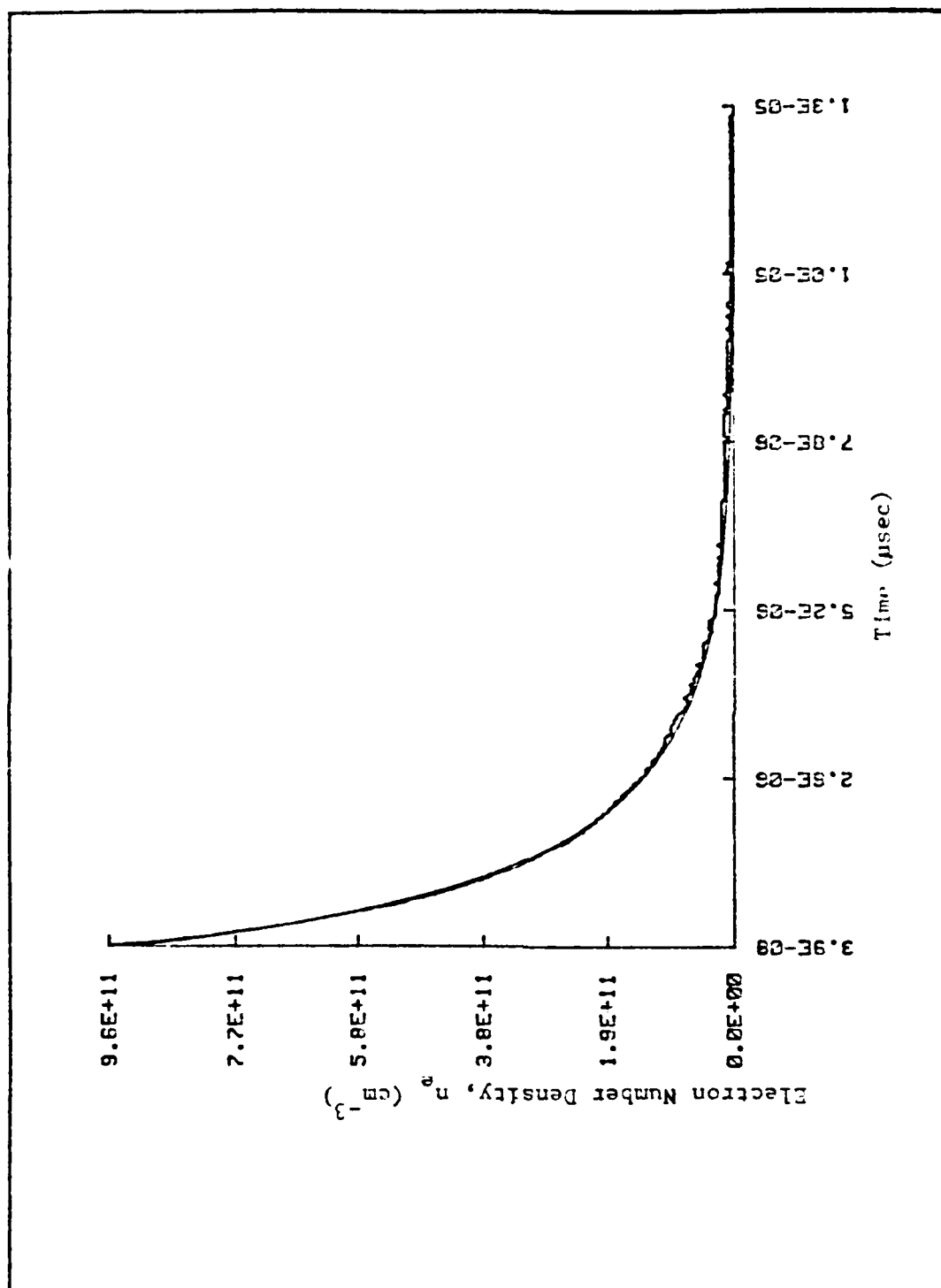
Figure 17. Computer Fit to Excerpted Current Decay Curve

Measurements in C_2F_6/CH_4

Tables IV and V, in Appendix B, list the properties of the 700 torr 1/7550, C_2F_6/CH_4, gas mixture used in this study. The system operating conditions are the same as those used for the pure CH_4 experiment, i.e, e-beam prefoil currents of 400 mA and 1 A and discharge voltages spanning the range of the electrode power supply. The analog results from mass analysis are shown in Appendix C, both before e-beam pulsing and after 251,000 e-beam pulses. Any changes in the amplitude of the masses observed between measurements could be attributed to the fluctuations in the mass analyzer's output during the measurement of up to 80%. Therefore only the types of ion species present were of any significant value. The species present before and after e-beam pulsing are shown in Figures 21 thru 32, in Appendix C. As seen, there was no significant change in the masses present before and after pulsing. However, a more sensitive device may have given more reliable results, which may have shown the type and amount of change in the masses present.

Attachment Rate vs E/N. Figure 18 shows the computed attachment rates vs E/N for both the C_2F_6/CH_4 gas mixture and for pure CH_4. At low E/N (< 3 T_d), the attachment rate appears to increase dramatically, both for the gas mixture and for pure CH_4. Although the increase might be associated with CH_4, it is more likely that the fitting routine was inaccurate due to the effects of the e-beam on the discharge current decay curve. Also, as was shown in Figure (3) of

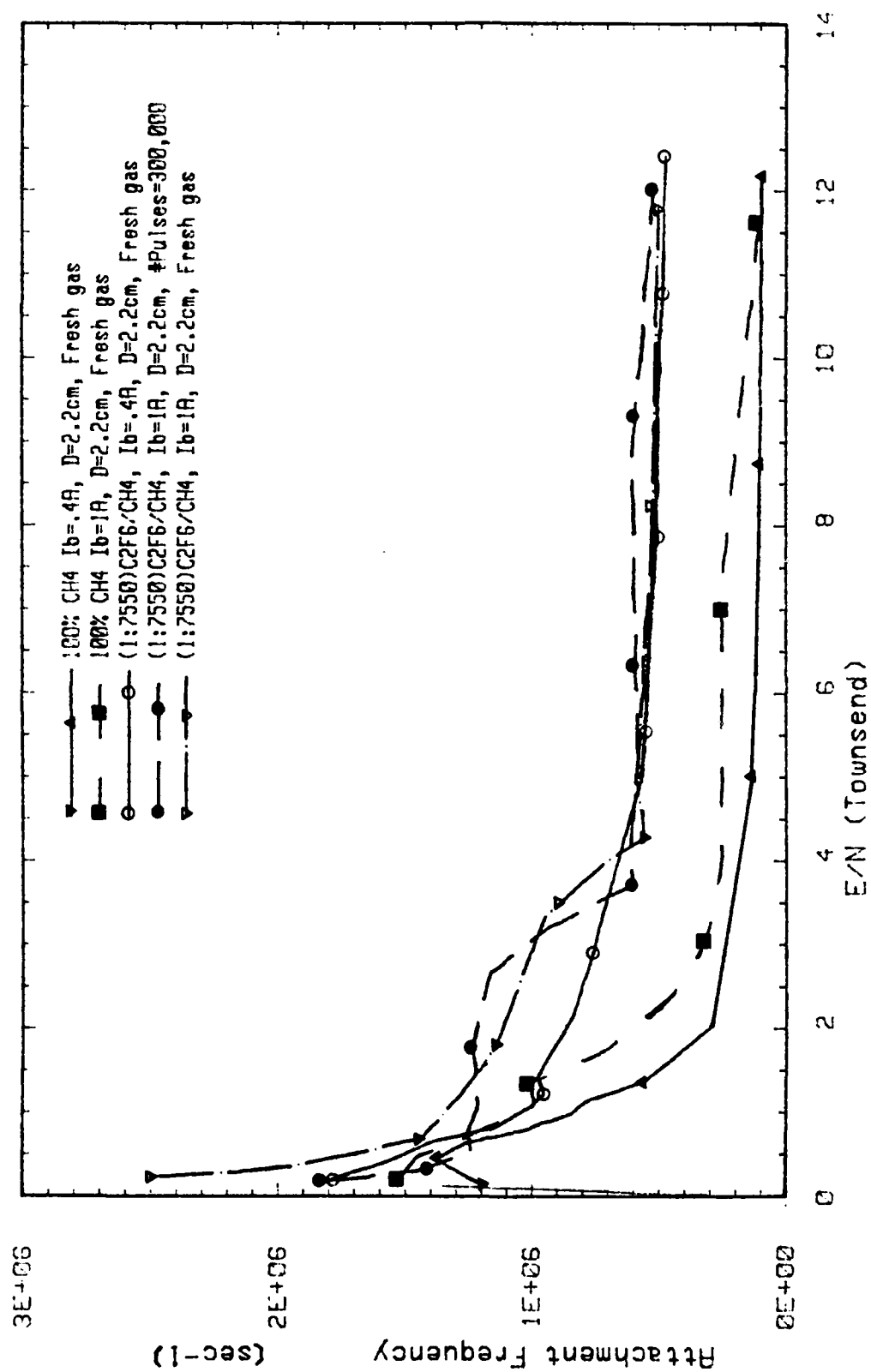Figure 18. Plot of Attachment Frequency vs E/N for Pure Methane and Methane Plus the Attaching Gas C_2F_6, at a Temperature of 294°K and Pressure of 700 Torr

Section II, the recombination rate increases dramatically at lower E/N further compounding the effect of the slow e-beam decay in this region.

At higher E/N values ($E/N > 4$ T_d), the attachment rates appear to level out and show a marked difference in attachment between pure CH_4 and the gas mixture. Figure 19 represents the discharge current for both experiments using the same operating conditions. Again the effects of a higher attachment rate are observed by a lowering of the steady-state current and an increased rate of decay for the gas mixture than for the pure CH_4. The attachment rate for the C_2F_6/CH_4 gas mixture levels out at an attachment rate of 4.5×10^5 sec^{-1} which is an order of magnitude higher than expected from drift tube measurements [13:1655-1656]. However, the attachment rate of pure CH_4 at the high E/N values is 1×10^5 as suggested by Kline [3:44] and Bletzinger [11:83]. Since the results by Kline and Bletzinger were from e-beam measurements similar to those in this study, the results here for both the pure gas and the gas mixture are thought to be reliable. There are at least two explanations for the difference between the present measurements and those in the previously mentioned swarm experiments: (1) the swarm experiments were not performed under actual e-beam switch conditions, so that high current discharge effects on the attachment rate were neglected, and (2) the apparent attachment rate of C_2F_6 may appear higher due to chemical changes in the gas mixture from dissociation

61
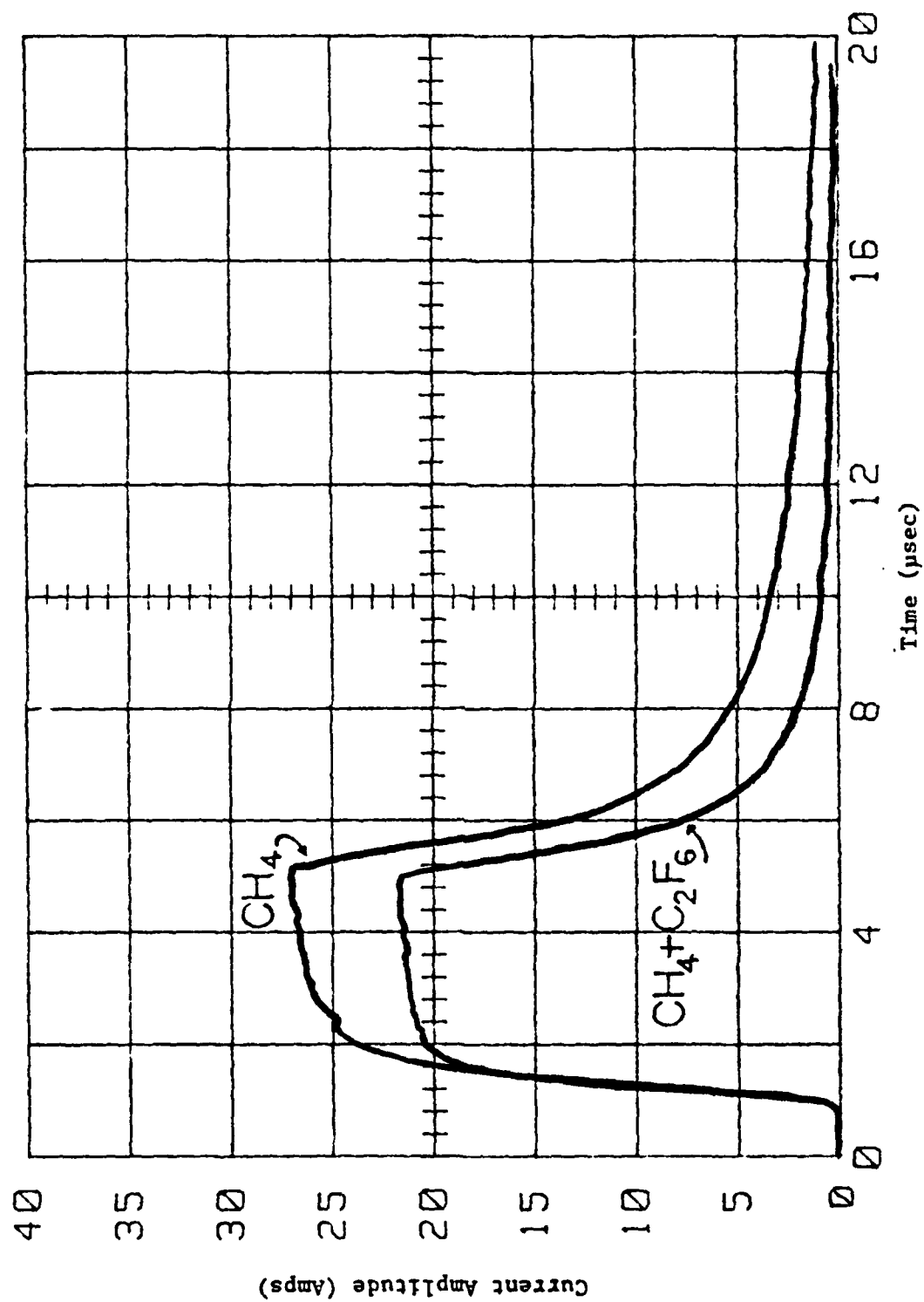
Figure 19. Comparison of Discharge Current for CH_4 and C_2F_6/CH_4 Gas Mixture

62

or ionization into gas products that are highly electronegative, such as fluorine.

Attachment Rate vs Number of Switch Operations. Figure 20 portrays the attachment rate of the C_2F_6/CH_4 gas mixture described above vs number of gas discharges under the following operating conditions:

1. E-beam prefoil current of 1 A

2. E-beam voltage of 175 kV

3. Electrode potential difference of 10 kV

4. Electrode separation of 2.2 cm

5. Pulse width of 4-μsec

Except for minor excursions of less than 10% which could be attributed to equipment and/or curve fitting errors, the attachment rate remained essentially unchanged over 300,000 pulses. This tends to confirm the prediction that the rate of dissociation due to the operation of the e-beam switch is negligible for large, circulating gas-flow loops.
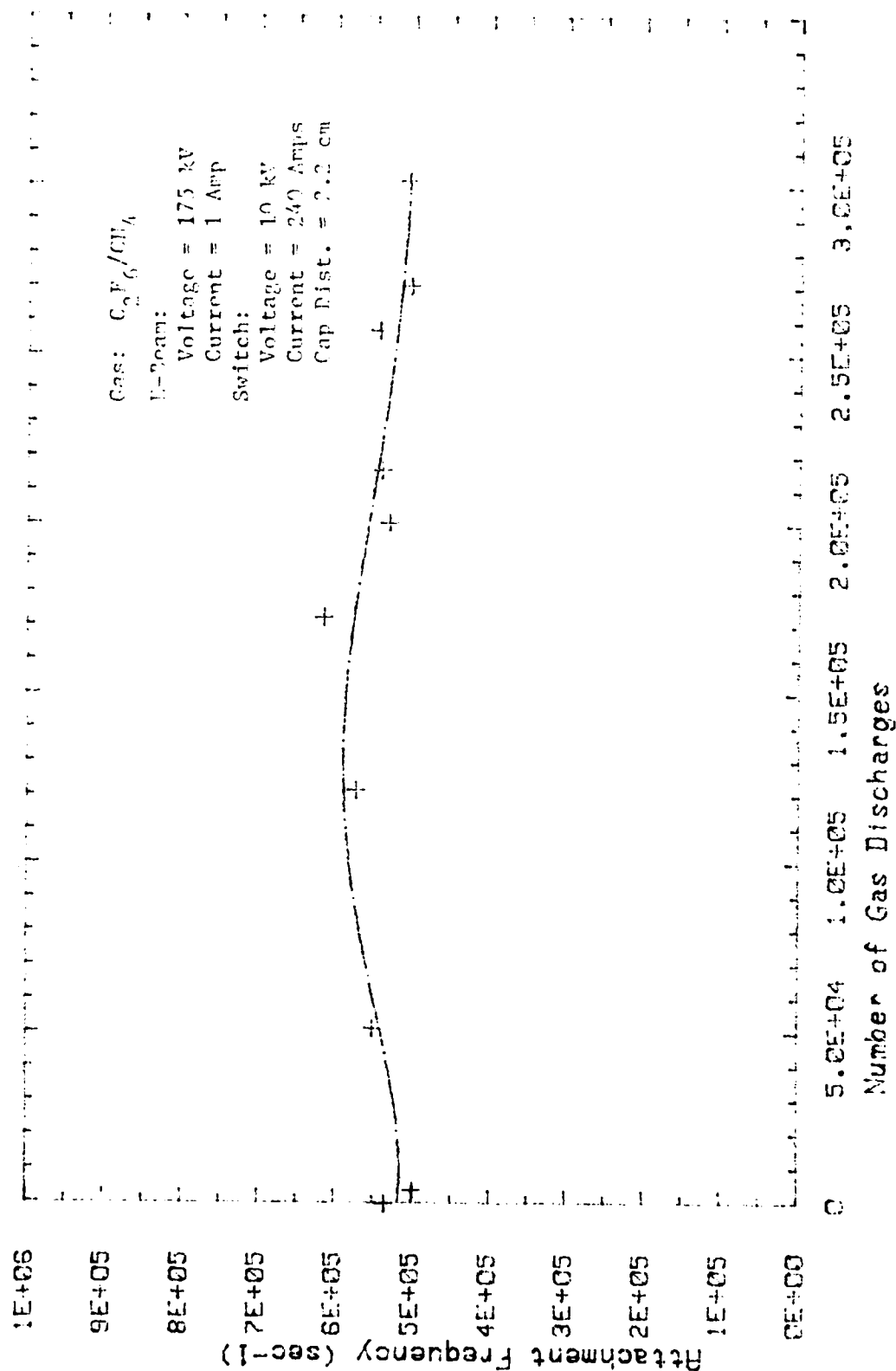
Figure 20. Plot of Attachment Rate vs Number of Discharges

VI   Conclusions and Recommendations

An atmospheric pressure gas mixture of 0.1/755, C_2F_6/CH_4 in a closed-cycle gas flow loop was subjected to e-beam-sustained gas discharges over an E/N range of .1 to 13 Townsend and e-beam prefoil currents of 400 mA and 1 A. An analytic solution of the electron lifetime equation was fit to the current decay curve to obtain the attachment rate for the gas mixture. The calculated attachment rate was 5×10^5 sec^{-1} for the E/N range of 3 to 13 Townsend. However, the attachment rate for .2 to 3 Townsend was inconclusive due to the effects of a slowly decaying e-beam pulse on the current decay. The attachment rate values for pure methane obtained in a similar way and over the same operating ranges were in close agreement with previous gas discharge experiments. Therefore, the attachment rates for the gas mixture are expected to be reliable, although higher than values obtained in swarm studies.

The dissociation rate for the attaching gas was determined not to be significant for large volume closed-cycle gas flow loops. However, the actual rate of dissociation was not experimentally determined. The primary method used to determine the dissociation rate, using a residual gas analyzer, had an uncertainty factor much greater than the expected dissociation rate. The secondary method, monitoring the change in attachment rate, was more reliable and indicated very little dissociation occurring.

65

However, it was not conclusive, since some of the dissociation products could be highly electronegative, such as fluorine, which would maintain the attachment rate artificially. If small dissociation rates must be determined or real time analysis is important for future applications, then additional experiments using laser spectroscopy or a much more sensitive and stable mass analyzer should be used.

The cathode-fall voltages measured in this study were predicted to be accurate to within 20%. The cathode-fall is a significant portion of the discharge voltage and so affects the value of E/N in the positive column region, the resulting drift velocity of electrons, and finally the value of n_{eo} calculated for the gas. Therefore, future attempts should be directed toward accurately determining the cathode-fall voltage as a function of E/N and addressing the oscillation problems encountered in the gas discharge.

This experiment was limited to a very low percentage of C_2F_6 (0.013%), still the current decay was fast enough to be affected by the e-beam decay. Therefore, either a computer routine to compensate for the e-beam decay in the fitting procedure, or a much faster decaying external ionization source is suggested for future gas discharge studies. Either of these changes to the present procedure would allow greater accuracy in determining the attachment and recombination rates at low E/N values.

Appendix A

Error Analysis

The significant errors found due to the mass analyzer in measuring the change in gas composition have already been discussed in the body of the report. The equipment errors that propagate through the system can be calculated using error analysis techniques, such as, those presented by Bevington [21:64]. For the present system the errors due to the equipment were computed using the following equipment error list:

1. Electrode area ($\pm 1\%$)

2. Pulse Transformer ($\pm 1\%$)

3. Oscilloscope ($\pm 2\%$)

4. Digitizer ($\pm 2\%$)

5. Digital Voltmeter (.06% full scale)

6. Plotter (± 0.025 mm)

7. Drift velocity (5%)

Using the data in the above list, the worst case uncertainty for E/N would be approximately 5% due to equipment. However, since the cathode-fall (see body of report) was accurate to only 20%, the mean error for E/N is approximately 21%. For the drift velocity, the maximum error can be assumed to be the 5% given above plus the 21% in E/N or 26% error. After analyzing the error propagation, it was concluded that a better way of measuring the cathode-fall should be found. Otherwise, the accuracy of the present

method for obtaining the attachment rates in e-beam studies may not yield sufficiently reliable data for some applications.

Neglecting the error due to the cathode-fall voltage, the computer generated curve fit was expected to be accurate to within ±5%. Therefore, for this study, the cathode-fall measurements determined through experiment were assumed accurate to allow some point of reference in calculating the attachment rates.

Appendix B

Tables of Discharge Data

TABLE II

Gas Discharge results for CH_4 (e-beam current is 400 mA)

E/N (Td)	Discharge		n_{eo} $(\times 10^{12})$ (cm^{-3})	W_d $(\times 10^6)$ (cm/sec)	β $(\times 10^5)$ (sec^{-1})	Cathode-Fall (Volts)
	Voltage (Volts)	Current (Amp)				
.17	394	1.65	.19	.71	11.9	321
.45	611	10.1	.34	2.48	13.8	382
.63	775	24.1	.58	3.49	12.6	457
.80	960	43.8	.81	4.49	10.2	557
.93	1170	72.1	1.10	5.53	8.42	674
1.1	1340	102	1.40	6.20	7.79	762
1.38	1560	103	1.20	7.03	5.58	858
2.00	1980	111	1.00	9.16	3.00	964
2.82	2400	115	.94	10.10	2.44	971
4.97	3340	123	1.00	10.00	1.38	831
7.76	5200	141	1.30	8.73	1.04	1277
9.78	7140	151	1.60	7.78	1.02	2199
12.2	8969	166	1.90	7.11	.95	2800

TABLE III

Gas Discharge results for CH_4 (e-beam current is 1 A)

E/N (Td)	Discharge		n_{eo} $(\times 10^{12})$ (cm^{-3})	W_d $(\times 10^6)$ (cm/sec)	β $(\times 10^5)$ (sec^{-1})	Cathode-Fall (Volts)
	Voltage (Volts)	Current (Amp)				
.20	391	3.88	.316	1.02	15.2	290
.31	579	20.3	1.00	1.68	15.0	420
.49	756	49.6	1.50	2.67	14.5	510
.70	933	87.7	1.90	3.90	12.6	580
1.08	1170	132.8	1.80	5.98	9.94	620
1.36	1320	166.4	2.00	6.94	10.0	630
1.75	1530	170.0	1.70	8.29	7.06	640
2.56	1970	178.5	1.50	9.90	3.93	670
3.24	2410	184.8	1.50	10.40	2.98	770
4.00	3320	197.7	1.60	10.20	2.54	1290
4.60	4880	220.3	1.76	10.10	2.55	2550
7.23	6660	242.2	2.20	9.00	2.56	3000
11.9	8450	265.6	3.00	7.20	.97	2425

TABLE IV

Gas Discharge results for C_2F_6/CH_4 (e-beam current is .4 A)

E/N (Td)	Discharge		n_{eo} ($\times 10^{12}$) (cm^{-3})	W_d ($\times 10^6$) (cm/sec)	β ($\times 10^5$) (sec^{-1})	Cathode-Fall (Volts)
	Voltage (Volts)	Current (Amp)				
.17	420	2.5	.24	.86	18.1	330
.38	560	9.3	.38	2.04	15.7	370
.62	770	19.4	.47	3.43	14.0	460
.83	1040	32.3	.58	4.67	11.5	620
1.02	1220	51.5	.75	5.73	10.3	710
1.23	1430	71.2	.91	6.48	9.50	810
1.39	1570	89.4	1.1	7.03	9.80	870
2.13	2060	102	.89	9.50	8.30	980
3.02	2490	104	.84	10.3	7.50	960
5.03	3380	111	.92	10.0	5.70	835
7.82	5280	119	1.1	8.70	5.10	1330
9.72	7130	125	1.3	7.80	4.97	2210
12.5	9060	128	1.5	7.60	4.70	2750

TABLE V

Gas Discharge results for C_2F_6/CH_4 (e-beam current is 1 A)

E/N (Td)	Discharge		n_{eo} ($\times 10^{12}$) (cm^{-3})	W_d ($\times 10^6$) (cm/sec)	β ($\times 10^5$) (sec^{-1})	Cathode-Fall (Volts)
	Voltage (Volts)	Current (Amp)				
.19	422	21.3	1.8	.97	18.3	318
.31	600	44.0	2.2	1.67	14.3	431
.52	813	71.2	2.1	2.84	12.4	534
.78	1020	104.0	2.0	4.37	12.6	599
1.11	1230	137.0	1.9	6.09	12.1	632
1.31	1348	173.0	2.1	6.78	12.2	640
2.67	2121	182.0	1.5	10.0	11.6	680
3.22	2547	186.0	1.5	10.4	9.3	807
3.73	3410	195.0	1.6	10.3	6.0	1393
4.06	4516	201.0	1.6	10.2	6.1	2324
4.95	5477	206.0	1.7	10.0	5.8	2804
8.29	7414	216.0	2.1	8.48	6.1	2933
12.0	9375	224.0	2.6	7.15	5.2	2893

Mass Analyzer Results

TABLE VI

Masses Present in Pure CH_4 at 1 ATM

Molecule	AMU
CH	13
CH_2	14
CH_3	15
O, CH_4	16
C_2H_2	26
CO, C_2H_4	28
CH_3CH_2	29
O_2, CH_3OH	32
C_3H_5	41
CH_3CO	43

The following graphs are the analog representation of the atomic mass units (amu) for the gas mixture 1/7550, C_2F_6/CH_4, at 700 torr total pressure. Figures 21 thru 26 are prior to e-beam operation and Figures 27 thru 32 are after 250,000 four-microsecond pulses with an E/N of 13 Townsend and an e-beam current of 1 A. The representations are from actual measurements using the Inficon IQ 200 residual gas analyzer.
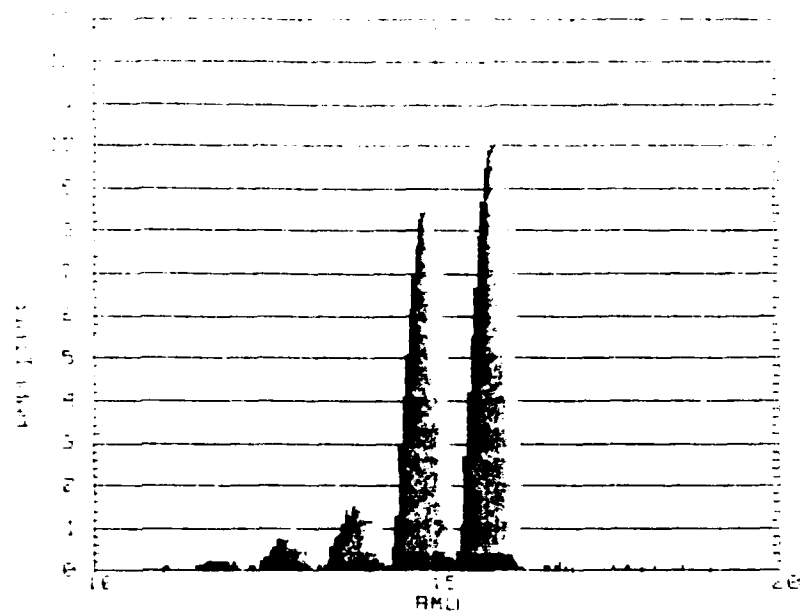
24 Nov -471 00:00:00
WITH SPAN: 10   ST MASS: 10   GAIN: 10   DWELL: 64
ELECT MULT: 1050

Figure 21

WITH SPAN: 20   ST MASS: 20   GAIN: 10   DWELL: 512
ELECT MULT: 1500

Figure 22.

Figure 21

Figure 22.

72

WITH SPAN: 20   ST MASS: 31   GAIN: 9   DWELL: 512
ELECT MULT: 2200

Figure 23.

WITH SPAN: 20   ST MASS: 45   GAIN: 9   DWELL: 512
ELECT MULT: 2800

Figure 24.

73

WITH SPAN: 40   ST MASS: 69   GAIN: 10   DWELL: 512
ELECT MULT: 2000

Figure 25.

WITH SPAN: 40   ST MASS: 100   GAIN: 10   DWELL: 4096
ELECT MULT: 3000

Figure 26.
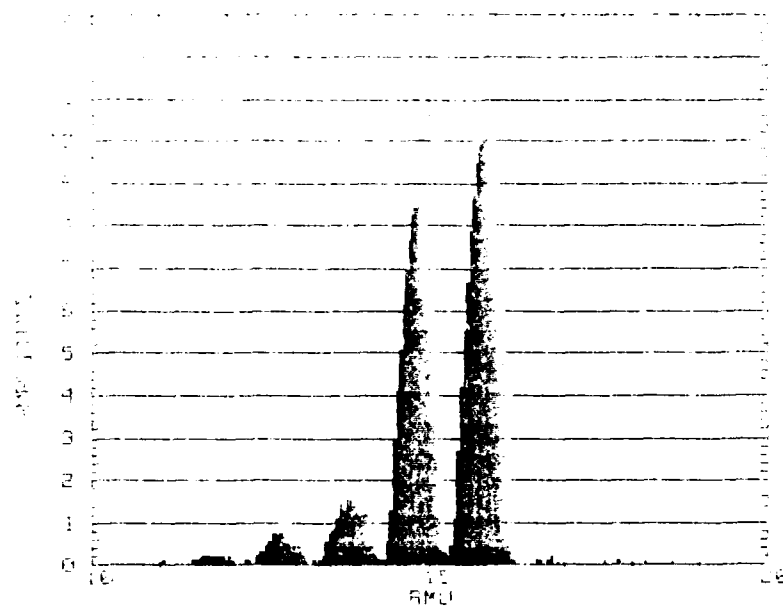
74

WITH SPAN: 10   ST MASS: 10   GAIN: 10   DWELL: 64
ELECT MULT: 1050

Figure 27.

WITH SPAN: 20   ST MASS: 20   GAIN: 9   DWELL: 256
ELECT MULT: 2100

Figure 28.

WITH SPAN: 20   ST MASS: 35   GAIN: 9   DWELL: 512
ELECT MULT: 2800

Figure 29.
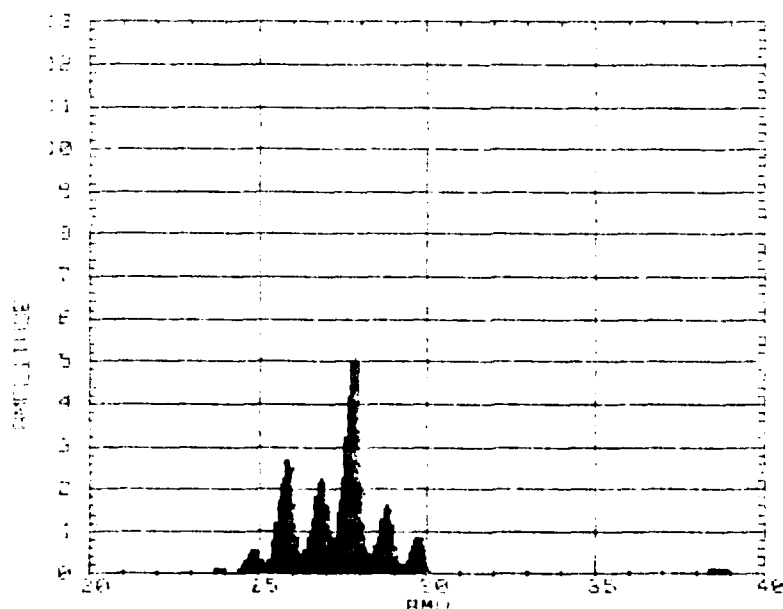

WITH SPAN: 20   ST MASS: 50   GAIN: 9   DWELL: 512
ELECT MULT: 3000

Figure 30.

76

WITH SPAN: 40   ST MASS: 60   GAIN: 10   DWELL: 512
ELECT MULT: 2900

Figure 31.

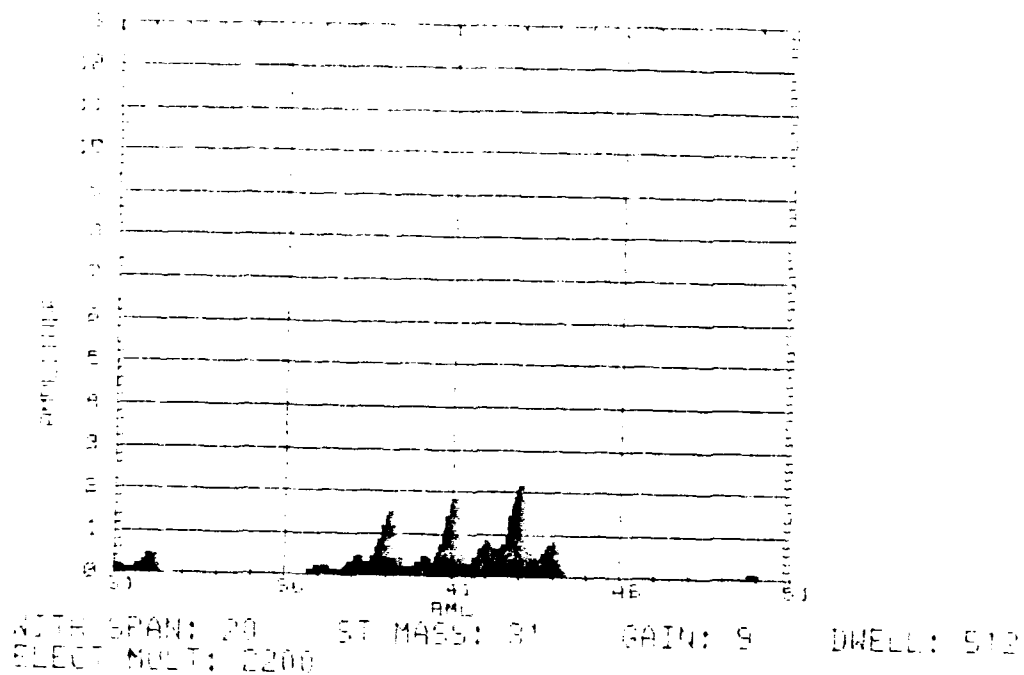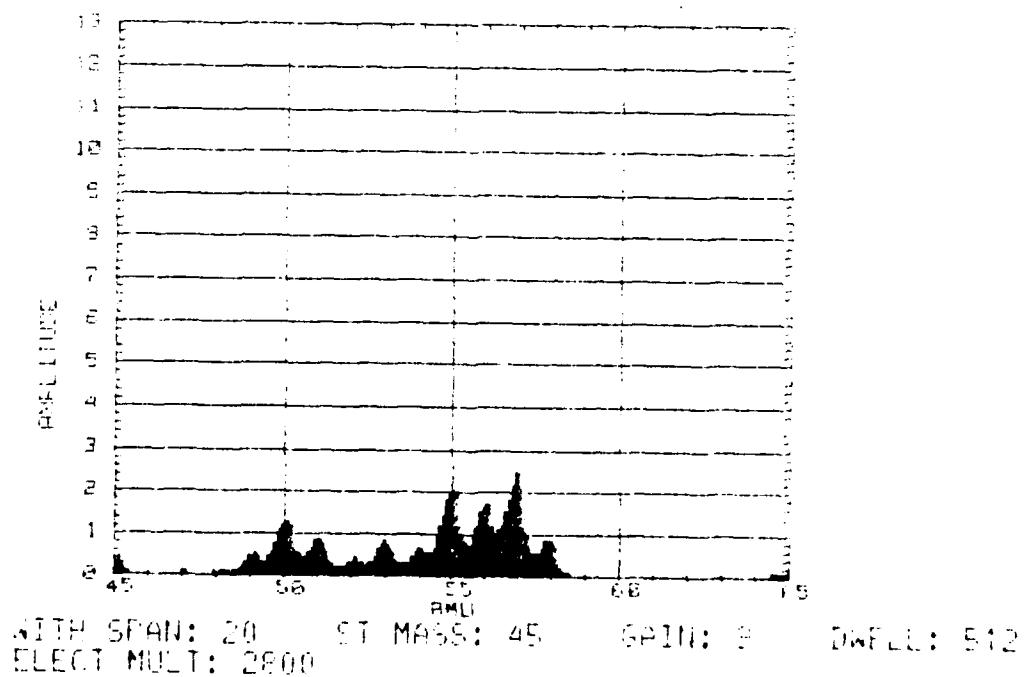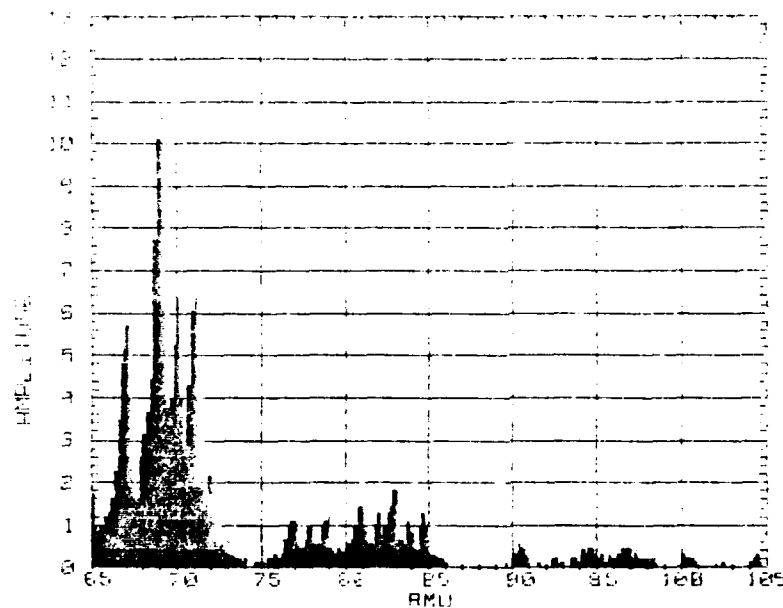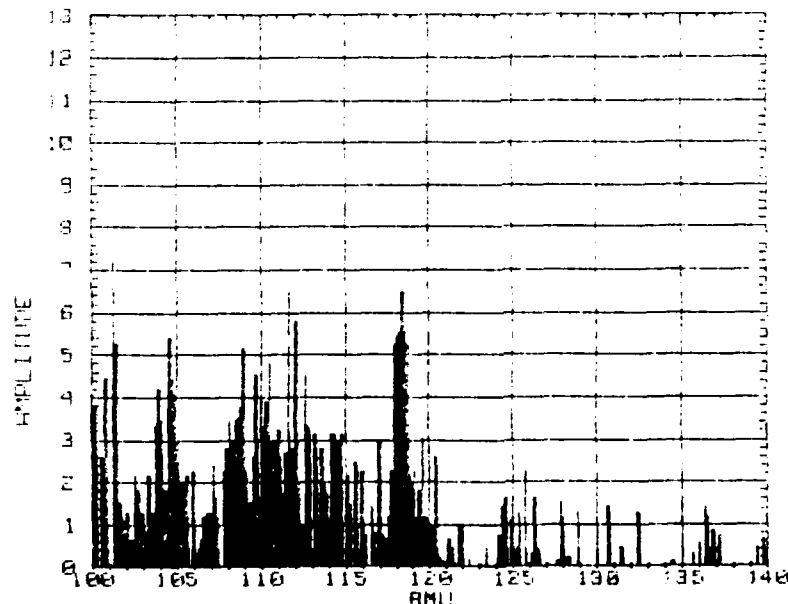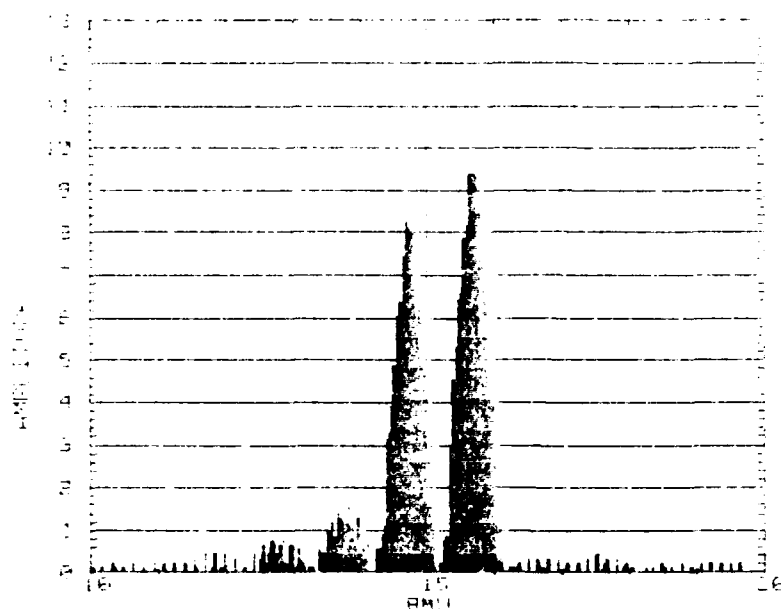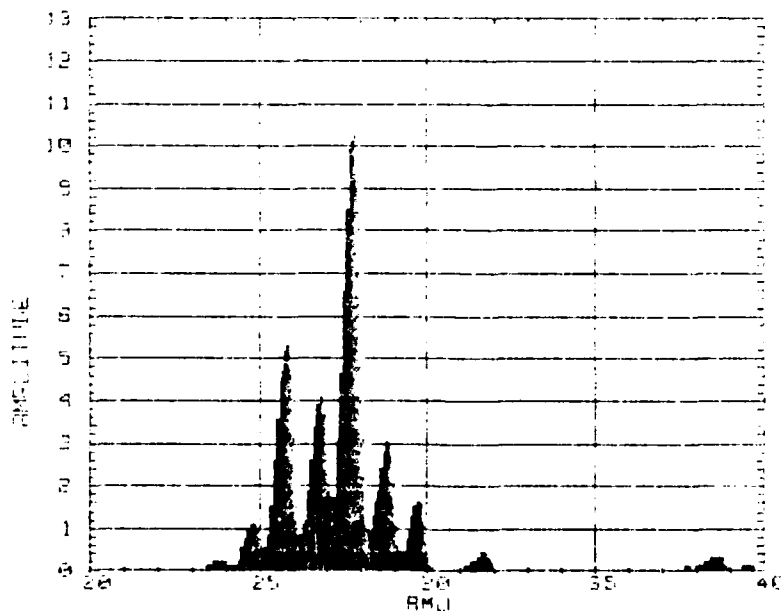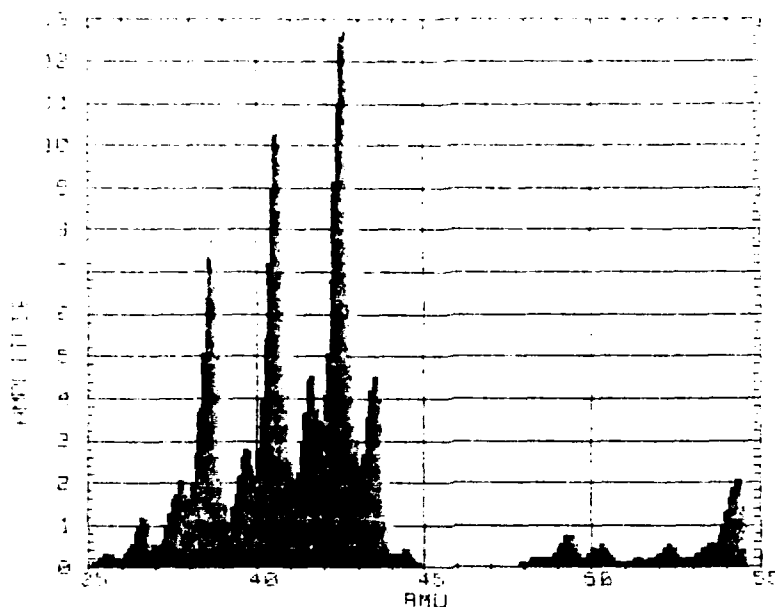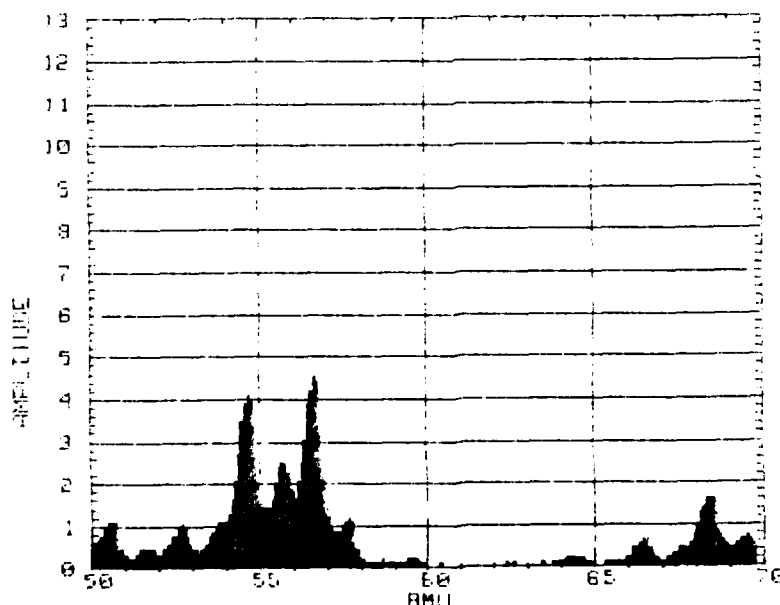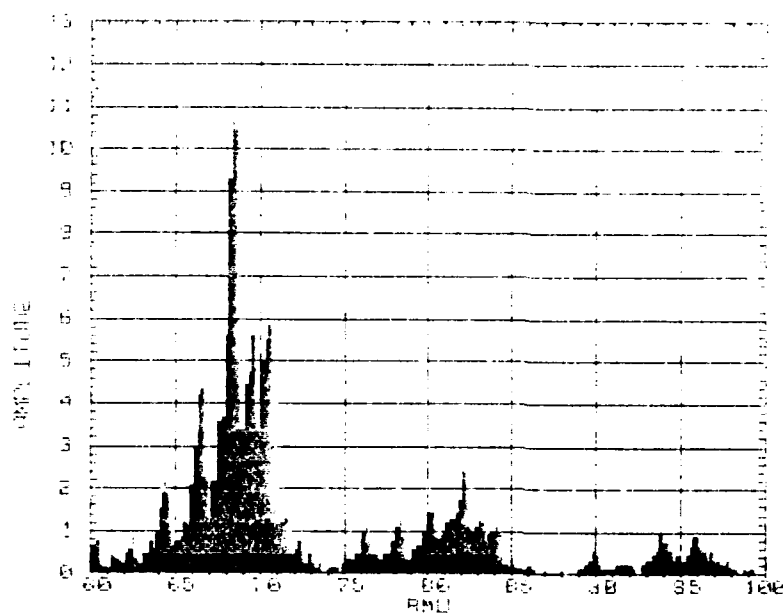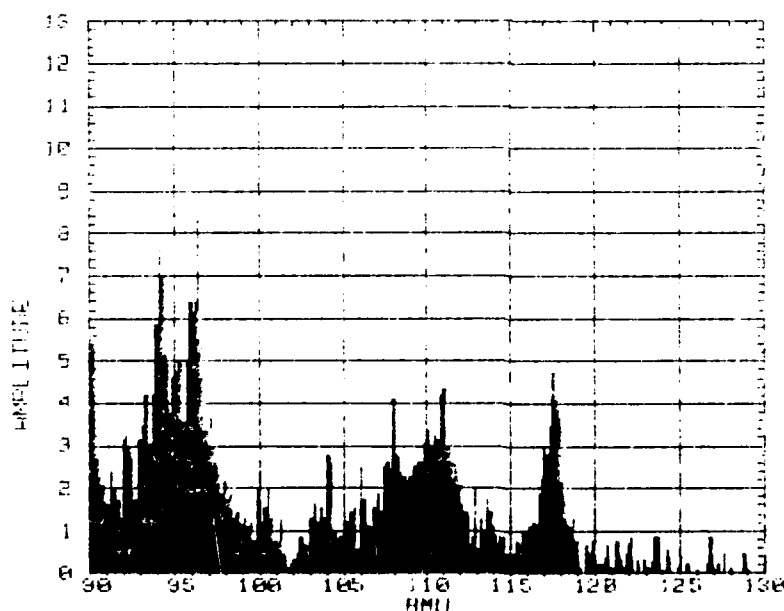WITH SPAN: 40   ST MASS: 90   GAIN: 11   DWELL: 1024
ELECT MULT: 3000

Figure 32.

Bibliography

1. Burton, J. K. and others. "Inductive Storage--Prospects for High Power Generation," Proceedings 2nd IEEE International Pulsed Power Conference. 284-286. IEEE Press, New York, 1979.

2. Schneider, Capt Greg R. Investigation of Electron Loss Processes in $CO_2/He/N_2$ Electric Discharges. MS thesis, GEP 80D-5. School of Engineering, Air Force Institute of Technology (AU), Wright-Patterson AFB, Ohio, December 1980 (AD-A094 398).

3. Dzimianski, J. W., L. E. Kline. High Voltage Switch Using Externally Ionized Plasmas: Final Report, 26 June 1978-- 21 December 1979. Contract F33615-78-C-2010. Westinhouse Electric Corporation, Baltimore Md, April 1980 (AFWAL-TR-80-2041).

4. Hunter, S. R. and others. "Transport Properties and Dielectric Strengths of Gas Mixtures for Use in Diffuse Discharge Opening Switches," Proceedings of the 4th International Symposium on Gaseous Dielectrics. IEEE Press, New York, 1984.

5. Bletzinger, P. "Scaling of Electron Beam Switches," Proceedings of the IEEE International Pulsed Power Conference. 37-40. IEEE Press, New York, 1983.

6. Douglas-Hamilton, D.H. "Recombination Rate Measurements in Nitrogen," Journal of Chemical Physics, 58:4820-4823 (June 1973).

7. Howatson, A.M. An Introduction to Gas Discharges (Second Edition). New York: Pergamon Press, 1976.

8. Von Engel, A. Ionized Gases (Second Edition). London: Oxford University Press, 1965.

9. Petrovic', Z.Lj. and others. "Model Calculations of Negative Differential Conductivity in Gases," Australian Journal of Physics, 37: 23-34 (May 1984).

10. Robson, R.E. "Generalized Einstein Relation and Negative Differential Conductivity in Gases," Austrailian Journal of Physics, 37: 35-44 (May 1984)

11. Bletzinger, P. "Electron Beam Switching Experiments in the High Current Gain Regime," Proceedings of the 3rd IEEE International Pulsed Power Conference. 81-84. IEEE Press, New York, 1981.

12. Kline, L. E. "Performance Predictions for E-Beam Controlled On/Off Switches," IEEE Transactions on Plasma Science, PS-10: 224-233. (December 1982).

13. Hunter, S.R. and L.G. Christophorou. "Electron Attachment to the Perfluoroalkanes n-$C_N F_{2N+2}$ (N=1-6) Using High Pressure Swarm Technique," Journal of Chemical Physics, 12: 6150-6164 (June 1984).

14. Duncan, C.W. and I.C. Walker. "Collision Cross Sections for Low Energy Electrons in Methane," Journal of the Chemical Society, Faraday Transactions, 68: 1514 (Aug 1972).

15. Pages, L. and others. "Energy Loss, Range and Bremsstrahlung Yield for 10 keV to 100 MeV Electrons in Various Elements and Chemical Compounds," Atomic Data, 4: 1-127 (April 1974)

16. Bletzinger, P., Senior Engineer, Energy Conversion Branch. Personal interview. AFWAL/POOC-3. Wright-Patterson AFB, Ohio, 30 May 84.

17. Winters, H.F. "Total Dissociation Cross Section of CF_4 and Other Fluoroalkanes for Electron Impact," Physical Review A, 25 (3): 1420-1430 (March 1982).

18. Hallada, M.R. and others "Application of Electron-Beam Ionized Discharges to Switches-A Comparison of Experiment With Theory," IEEE Transactions on Plasma Science, PS-10: 218-224 (December 1982).

19. Kristiansen, M. and K.H. Schoenback. Workshop on Repetitive Opening Switches: Final Report, 28-30 January 1981. Contract DAAG29-76-D-0100. Texas Tech University, Lubbock Tx, April 1981.

20. IQ-200 Mass Analyzer. Technical Manual. Inficon Leybold-Haraeus, E. Syracuse NY, July 1980.

21. Bevington, P.R. Data Reduction and Error Analysis for the Physical Sciences. New York: McGraw-Hill Book Co., 1969.

VITA

Lieutenant Verl R. Wilson was born on 1 January 1948 in Rigby, Idaho. He graduated from Rigby High school in 1966 and recieved his under graduate degree in electrical engineering from Arizona State University in December 1980. Upon graduation he attended Officer's Training School (OTS) in Texas, where he was a distinquished graduate. After OTS he worked in Air Force logistics for the F-16 System Managers Office, Avioics Section, at Hill AFB, Utah. Lieutenant Wilson had served a total of 18 years active duty with the Air Force upon entering the School of Engineering, Air Force Institute of Technology, in May 1983.

Permanent Address: 2814 E. Chicago
Caldwell, Idaho 83605

REPORT DOCUMENTATION PAGE

1. REPORT SECURITY CLASSIFICATION UNCLASSIFIED	1b. RESTRICTIVE MARKINGS
2a. SECURITY CLASSIFICATION AUTHORITY	3. DISTRIBUTION/AVAILABILITY OF REPORT Approved for public release: IAW AFR 190-17.
2b. DECLASSIFICATION/DOWNGRADING SCHEDULE	Professional Development (AIC)
4. PERFORMING ORGANIZATION REPORT NUMBER(S) AFIT/GEP/PH/	5. MONITORING ORGANIZATION REPORT NUMBER(S)

6a. NAME OF PERFORMING ORGANIZATION School of Engineering	6b. OFFICE SYMBOL (If applicable)	7a. NAME OF MONITORING ORGANIZATION
6c. ADDRESS (City, State and ZIP Code) Air Force Institute of Technology Wright Patterson AFB, Ohio 45433		7b. ADDRESS (City, State and ZIP Code)

8a. NAME OF FUNDING/SPONSORING ORGANIZATION Wright	8b. OFFICE SYMBOL (If applicable)	9. PROCUREMENT INSTRUMENT IDENTIFICATION NUMBER

8c. ADDRESS (City, State and ZIP Code) Wright Patterson AFB, Ohio 45433	10. SOURCE OF FUNDING NOS			
	PROGRAM ELEMENT NO	PROJECT NO.	TASK NO	WORK UNIT NO.

11. TITLE (Include Security Classification)
See box 19

12. PERSONAL AUTHOR(S)

13a. TYPE OF REPORT MS Thesis	13b. TIME COVERED FROM ___ TO ___	14. DATE OF REPORT (Yr, Mo, Day) 84 December	15. PAGE COUNT 98

16. SUPPLEMENTARY NOTATION

17	COSATI CODES		18. SUBJECT TERMS (Continue on reverse if necessary and identify by block number)
FIELD	GROUP	SUB. GR.	Electron, Attachment, Recombination, Perfluorocarbons, Optical Emission Field, Cross Section, Plasma, Gaseous Electronics, Streamer, Electric, Dissociation

19. ABSTRACT (Continue on reverse if necessary and identify by block number)

Title: ELECTRON ATTACHMENT, RECOMBINATION, AND DISSOCIATION RATES IN C_3F_8/CH_4 ELECTRIC DISCHARGES

Thesis Advisor: William F. Bailey, Lt. Col., USAF
Department of Engineering Physics

20. DISTRIBUTION/AVAILABILITY OF ABSTRACT UNCLASSIFIED/UNLIMITED ☐ SAME AS RPT ☐ DTIC USERS ☐	21. ABSTRACT SECURITY CLASSIFICATION UNCLASSIFIED
22a. NAME OF RESPONSIBLE INDIVIDUAL William F. Bailey, Lt. Col., USAF	22b. TELEPHONE NUMBER	22c. OFFICE SYMBOL

DD FORM 1473, 83 APR   EDITION OF 1 JAN 73 IS OBSOLETE.

This investigation determined the attachment and dissociation rates of the electronegative gas, C_2F_6, in a buffer gas of methane, CH_4, at atmospheric pressure when undergoing electron-beam sustained gas discharges. A non-linear least squares fit of the electron lifetime equation to the decay portion of the discharge current pulse indicates an attachment rate of 5×10^5 /sec^{-1} for a gas mixture ratio of 1/7550, C_2F_6/CH_4, and an E/N range of 3 to 13 Townsend. Results of the curve fit were inconclusive for E/N below 3 Townsend due to the effects of a slowly decaying electron-beam. Attempts were made to measure the dissociation rate of C_2F_6 as a function of discharge time for a ratio of E/N equal to 13 Townsend using a residual gas analyzer. The actual dissociation rate was not determined. However, it was confirmed that the dissociation of C_2F_6 due to the electron-beam ionization pulses and the corresponding gas discharge was not significant in large closed-cycle gas flow loops as proposed for pulsed power switching if E/N is held below 13 Townsend.

END